The C8ORF38 homologue Sicily is a cytosolic chaperone for a mitochondrial complex I subunit

Ke Zhang,[1] Zhihong Li,[2] Manish Jaiswal,[2,3] Vafa Bayat,[4,5] Bo Xiong,[4] Hector Sandoval,[2] Wu-Lin Charng,[4] Gabriela David,[4] Claire Haueter,[3] Shinya Yamamoto,[4] Brett H. Graham,[2,4] and Hugo J. Bellen[1,2,3,4,6,7]

[1]Program in Structural and Computational Biology and Molecular Biophysics, [2]Department of Molecular and Human Genetics, [3]Howard Hughes Medical Institute, [4]Program in Developmental Biology, [5]Medical Scientist Training Program, [6]Department of Neuroscience, and [7]Jan and Dan Duncan Neurological Research Institute, Baylor College of Medicine, Houston, TX 77030

Mitochondrial complex I (CI) is an essential component in energy production through oxidative phosphorylation. Most CI subunits are encoded by nuclear genes, translated in the cytoplasm, and imported into mitochondria. Upon entry, they are embedded into the mitochondrial inner membrane. How these membrane-associated proteins cope with the hydrophilic cytoplasmic environment before import is unknown. In a forward genetic screen to identify genes that cause neurodegeneration, we identified *sicily*, the *Drosophila melanogaster* homologue of human *C8ORF38*, the loss of which causes Leigh syndrome. We show that in the cytoplasm, Sicily preprotein interacts with cytosolic Hsp90 to chaperone the CI subunit, ND42, before mitochondrial import. Loss of Sicily leads to loss of CI proteins and preproteins in both mitochondria and cytoplasm, respectively, and causes a CI deficiency and neurodegeneration. Our data indicate that cytosolic chaperones are required for the subcellular transport of ND42.

Introduction

The vast majority of mitochondrial proteins (~99%) are encoded by nuclear genes, translated in cytoplasm, and imported into mitochondria via different pathways (Truscott et al., 2003). Previous studies have shown that proteins with internal mitochondrial targeting sequences (MTSs; IMTSs) are chaperoned by heat shock proteins (Young et al., 2001, 2003) in the cytoplasm. In addition, messages of many mitochondrial proteins of prokaryotic evolutionary origin localize to ribosomes in the vicinity of mitochondria for co-translational import into mitochondria (Marc et al., 2002; Garcia et al., 2007). However, other proteins, including many proteins that are part of the mitochondrial complex I (CI), do not fall into either of these categories. Most of them contain N-terminal MTSs (NMTSs) that are cleaved from the preproteins upon mitochondrial import. In addition, most CI subunits are of eukaryotic origin, and mRNAs encoding proteins of eukaryotic origin are translated on free cytosolic ribosomes (Marc et al., 2002). How these preproteins cope with the hydrophilic environment before their mitochondrial import is ill defined, possibly because they are not present in some model organisms, such as yeast.

CI (also known as NADH coenzyme Q oxidoreductase) is the largest protein complex in the electron transport chain (ETC). It is an integral membrane protein complex that resides in the mitochondrial inner membrane (Carroll et al., 2006) and consists of >40 subunits. Seven subunits are encoded by the mitochondrial genome, whereas the others are encoded in the nucleus (Lazarou et al., 2009). Many of these nuclear encoded subunits possess NMTSs but not IMTSs (Marc et al., 2002).

CI plays a central role in energy metabolism and regulation of reactive oxygen species (ROS) production (Owusu-Ansah et al., 2008; Owusu-Ansah and Banerjee, 2009). Cells with high energetic demands, such as neurons, are very sensitive to CI deficiency (de Souza-Pinto et al., 2008; Knott et al., 2008), and defects in CI function have been linked to elevated

Correspondence to Hugo J. Bellen: hbellen@bcm.edu

C. Haueter's present address is Anatomical Pathology Department, The Methodist Hospital Research Institute, Houston, TX 77030.

Abbreviations used in this paper: CI, complex I; CV, complex V; *da*, *daughterless*; ERG, electroretinogram; ETC, electron transport chain; GA, geldanamycin; IMTS, internal MTS; IP, immunoprecipitation; MTS, mitochondrial targeting sequence; NMTS, N-terminal MTS; PR, photoreceptor; ROS, reactive oxygen species; SD, synthetic defined; TEM, transmission EM; UAS, upstream activation sequence.

The Rockefeller University Press $30.00
J. Cell Biol. Vol. 200 No. 6 807–820
www.jcb.org/cgi/doi/10.1083/jcb.201208033

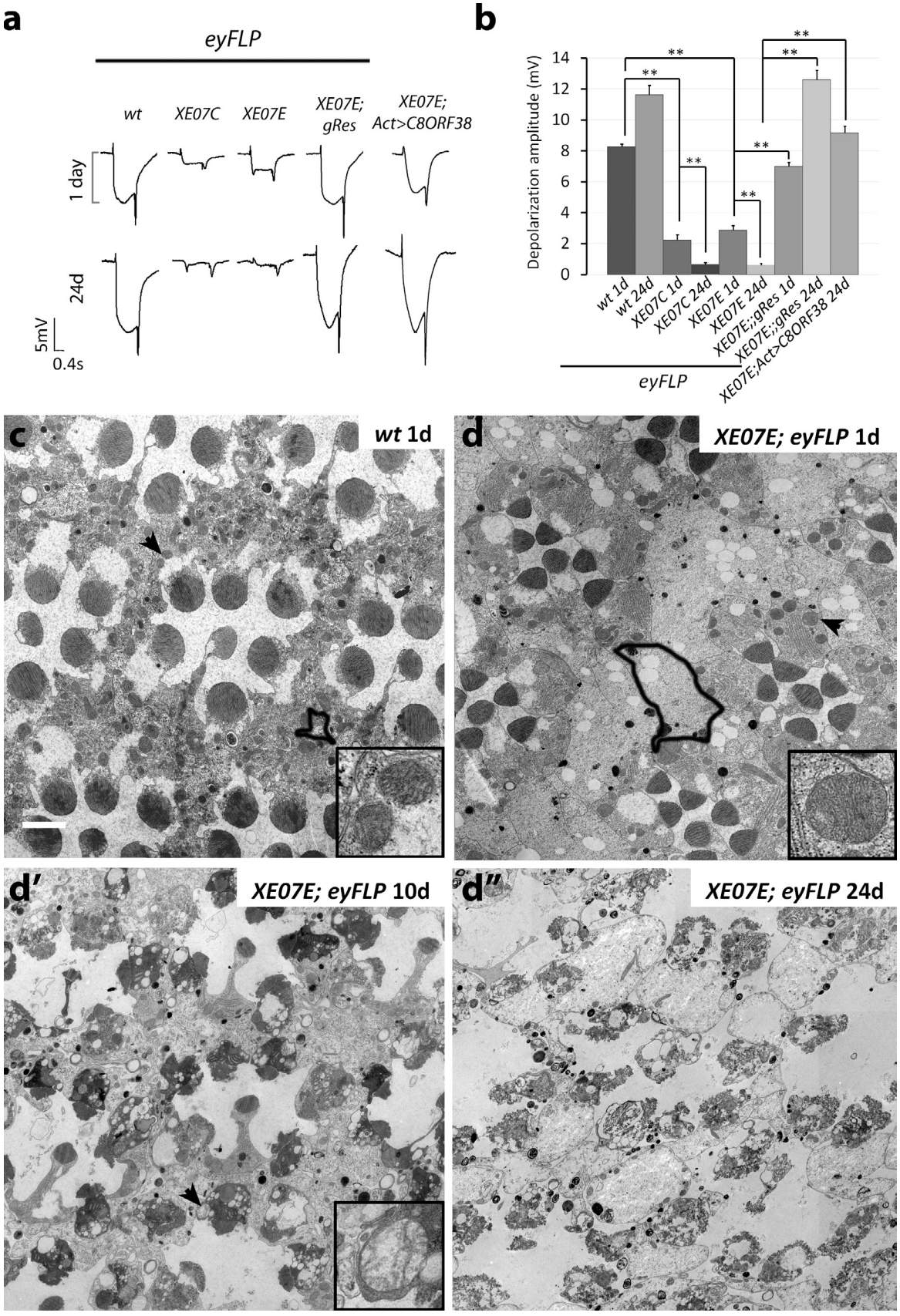

Figure 1. ***XE07* mutants display progressive neurodegenerative features in PRs.** (a) In response to a 1-s light pulse, 1-day-old *XE07* mutant flies display reduced amplitudes (bracket) when compared with wild type. Aging these flies causes the defects to worsen, and the ERG amplitudes are almost completely abolished after 24 d. This defect can be rescued by either a fly genomic construct or human *C8ORF38* cDNA. (b) Quantification of the depolarization amplitude in a. Data are presented as means ± SEM. **, $P < 0.01$, Student's *t* test. (c–d'') TEM sections of fly retinas. Mutant retinas (d) display normal

production of ROS and various neurodegenerative disorders, such as Alzheimer's disease, Parkinson's disease, and Leigh syndrome (Morris et al., 1996; Manczak et al., 2004; Clark et al., 2006; Morais et al., 2009).

In a recent study, Pagliarini et al. (2008) identified a mitochondrial CI assembly factor, *C8ORF38*. Knockdown of *C8ORF38* by RNAi in human fibroblasts resulted in decreased levels of CI subunits and reduced CI activity. In addition, two siblings who presented with Leigh syndrome, an early onset neurodegenerative mitochondrial disorder, were shown to harbor a homozygous splicing mutation in *C8ORF38* (Pagliarini et al., 2008; McKenzie et al., 2011). C8ORF38 has an NMTS and is localized to the mitochondrial matrix (McKenzie et al., 2011). Loss of C8ORF38 affects the stability, but not the synthesis, of ND1, a CI subunit encoded by the mitochondrial genome (Zurita Rendón and Shoubridge, 2012). However, the precise role of C8ORF38 remains elusive.

We isolated *sicily* mutations in an unbiased forward genetic screen in *Drosophila melanogaster*. *sicily* encodes the homologue of human C8ORF38. We show that Sicily interacts with cytosolic Hsp90 to chaperone a CI subunit, ND42, in the cytoplasm. In the absence of Sicily, CI activity is severely impaired, and ROS production is elevated. We also show that Sicily does not require its MTS for its function in CI assembly. Our data provide evidence that cytosolic chaperones regulate mitochondrial CI assembly by escorting a CI subunit in the cytoplasm before its mitochondrial import.

Results

XE07 mutations cause severe neurodegenerative phenotypes

To identify novel genes on the *Drosophila* X chromosome that cause a neurodegenerative phenotype, we performed a large forward mosaic genetic screen using the flippase/flippase recognition target system (Xiong et al.,2012; Yamamoto et al., 2012) and identified a complementation group, *XE07*, which exhibits degenerative electroretinogram (ERG) defects in clones. In response to a light pulse, 1-day-old flies display reduced amplitudes (Fig. 1, a [bracket] and b), when compared with wild-type tissue. Aging the flies causes the defects to worsen, and the ERG amplitudes are almost completely abolished after 24 d (Fig. 1, a and b), showing that the photoreceptors (PRs) deteriorate with age. To determine whether there is a progressive morphological demise of the PR, we performed transmission EM (TEM) on mutant retinas of flies of different ages. Newly eclosed flies with *XE07* mutant clones contain a normal number of rhabdomeres per ommatidium with the typical trapezoidal organization. However, the pigment cells that function as glial cells in the eye are vastly expanded and display highly aberrant morphological features (compare Fig. 1, d and c). Upon aging for 10 d, some rhabdomeres are missing, and many PRs appear rough and/or vacuolated. The cell bodies of PRs are packed with electron-dense particles (Figs. 1 d′ and S1 a). At day 24, the rhabdomeres are barely recognizable or missing (Fig. 1 d′′), whereas the wild-type retinas still exhibit intact structure (Fig. S1 b). Hence, loss of *XE07* causes a severe neurodegenerative phenotype. To assess whether this phenotype is light dependent, we raised the flies in complete darkness. Flies with mutant clones raised in darkness display less aberrant rhabdomeres per ommatidium than flies raised in a light/dark cycle (Fig. S1, a and c). Hence, the neurodegeneration associated with *XE07* occurs in both the presence and absence of light and is only delayed in the dark.

TEM also revealed defects associated with mitochondria. Mitochondria of newly eclosed mutants are enlarged when compared with mitochondria in wild-type tissue (Figs. 1, d, compare with c, arrowheads and insets; and S1 d). At day 10, the mutant mitochondria are swollen and vacuolated, with dissociated cristae (Fig. 1 d′, arrow and inset). At day 24, the overall morphology of PRs is so severely affected that one can hardly identify mitochondria (Fig. 1 d′′).

XE07 is the *Drosophila* homologue of human *C8ORF38*

To identify the molecular lesions of the *XE07* alleles, we performed duplication and deficiency mapping. A lethal *P* element insertion line (Bellen et al., 2004) affecting *CG15738* fails to complement the lethality of all six alleles, indicating that *XE07* corresponds to *CG15738* (Fig. S2 a). Sanger sequencing identified three nonsense mutations (A, E, and H), two deletions (C and G), and a mutation in a potential splicing site (B) in *CG15738* (Fig. 2 a). Mutant hemizygous males and transheterozygous females are pupal lethal (Fig. S2 b). Interestingly, mutant larvae have very extended larval stages and live for 7–10 d as third instars before pupation, whereas wild-type third instars typically pupate after 2 d. We therefore named our gene "*sicily*" for severe impairment of CI with lengthened youth (Fig. 2 d). Finally, the ERG and TEM of the lamina associated with the six alleles do not reveal an obvious allelic series (unpublished data), suggesting that all alleles are similar loss-of-function mutations. We therefore decided only to characterize two alleles: $sicily^{C}$ (loss of the promoter and first two exons) and $sicily^{E}$ (Q133X).

The human homologue of Sicily, C8ORF38, is a mitochondrial CI assembly factor. Patients with mutations in *C8ORF38* presented with Leigh syndrome and CI deficiency (Pagliarini et al., 2008). Similar to its human homologue, Sicily possesses a predicted NMTS (11 aa). 70% of the protein consists of an evolutionarily conserved domain with unknown function (Fig. S2 c, black bar). Despite its similarity to the predicted evolutionary origin of squalene and phytoene synthase (~40% based on Pfam prediction), several key amino acids conserved in most squalene and phytoene synthases are absent in this domain (Robinson et al., 1993), suggesting that it may not possess an enzymatic function.

differentiation of seven rhabdomeres at day 1, but the pigment cells (bolded black lines) are largely expanded compared with wild type (c). Mutant rhabdomeres are dissociated after aging for 10 d (d′), and the defect worsens with age (d′′). Arrows in c–d′ indicate mitochondria that are also boxed. The bolded lines depict the membrane of single pigment cells. Bar, 2 µm. The boxes containing mitochondria are 1 µm × 1 µm. *wild type* (*wt*): *FRT19A; eyFLP*.

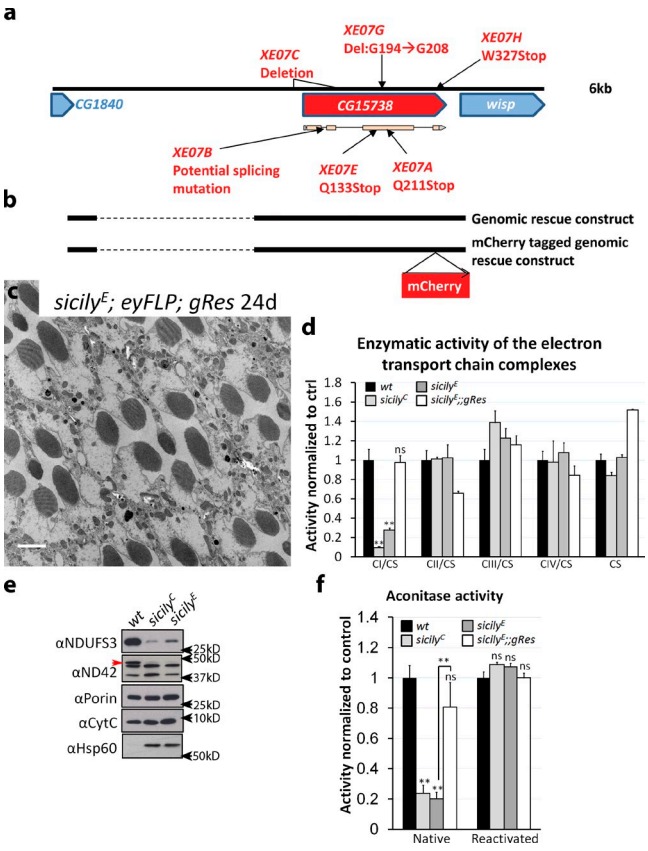

Figure 2. ***XE07* corresponds to *CG15738* (*sicily*), the fly homologue of human *C8ORF38*.** (a) Schematic representation of the molecular lesions of *XE07* alleles. (b) Extent of a genomic rescue construct and its mCherry-tagged version. The 5′ of *CG15738* contain seven repeats, and six of the repeats were lost (dashed lines) during PCR and other steps in the cloning. (c) TEM section of *sicily* mutant retina rescued by the genomic construct, aged for 24 d. The neurodegenerative phenotypes are fully rescued by the genomic rescue construct. Bar, 2 µm. (d) ETC assays show that mitochondrial complex I (CI) activity is severely compromised in *sicily* mutants. Data are presented as means ± SEM (**, $P < 0.01$, Student's *t* test, $n = 3$). (e) CI protein levels are severely reduced in *sicily* mutants. The arrowhead indicates the specific band for ND42. It also co-migrates with CI on Blue-Native PAGE. The middle band is detergent insoluble and does not appear on Blue-Native PAGE. The third band does not co-migrate with CI on Blue-Native PAGE (not depicted). (f) Aconitase assay. The aconitase assay was performed on purified mitochondria as previously described (Yan et al., 1997). Reducing reagents were used to reactivate native aconitase. Data are presented as means ± SEM (*, $P < 0.05$; **, $P < 0.01$; Student's *t* test; $n = 3$). *wild type* (*wt*): *FRT19A*. CytC, cytochrome *c*.

Genomic rescue constructs (Fig. 2 b) rescue the lethality (Fig. S2 b), ERG defects (Fig. 1, a and b), and retinal degeneration (Fig. 2 c) associated with the loss of *sicily* for all alleles. Ubiquitous expression of the *CG15738* cDNA using the GAL4/upstream activation sequence (UAS) system (Brand and Perrimon, 1993), driven by *daughterless* (*da*)-*GAL4* also rescues the lethality and phenotypes associated with all alleles (unpublished data), demonstrating that *sicily* indeed corresponds to *CG15738*. In addition, ubiquitous expression of human *C8ORF38* cDNA also rescues the lethality and ERG defects (Figs. 1, a and b; and S2 b), indicating that the function of *sicily/C8ORF38* is conserved between flies and human.

To determine whether *sicily* affects CI function, we performed the ETC assay and found that the CI activity is severely compromised in *sicily* mutants when compared with wild type (Fig. 2 d). To further test whether *sicily* affects the protein level of CI subunits, we immunoblotted purified mitochondria of *sicily* mutants with eight different antibodies raised against human CI subunits. Only two, NDUFS3 (Bratic et al., 2011) and NDUFA10 (ND42 in *Drosophila*), cross-reacted and were specific. Both NDUFS3 and ND42 are severely down-regulated in *sicily* mutants, whereas other mitochondrial proteins, including Porin (Graham et al., 2010) and cytochrome *c*, are unaltered or slightly increased (Fig. 2 e). These data indicate that *sicily* affects CI, in agreement with previous findings for *C8ORF38* (Pagliarini et al., 2008; McKenzie et al., 2011; Zurita Rendón and Shoubridge, 2012).

CI is responsible for most cellular ROS production in mitochondria (Brand, 2010), and impairment in CI activity often results in oxidative stress (Owusu-Ansah et al., 2008; Owusu-Ansah and Banerjee, 2009). To test this, we performed the aconitase assay, an indicator of ROS-mediated oxidative damage (Yan et al., 1997), and found that aconitase activity is severely decreased in *sicily* mutants, whereas the in vitro reactivated aconitase activity remains unaltered (Fig. 2 f), suggesting that the ROS levels are chronically increased in *sicily* mutant cells (Emptage et al., 1983). We also confirmed that the ROS level is increased in *sicily* mutant tissues based on MitoSOX staining (Invitrogen; unpublished data; Yarosh et al., 2008). ROS damages the proper folding of proteins that can activate Hsp60 (Yoneda et al., 2004; Bayat et al., 2012). As shown in Fig. 2 e, Hsp60 is up-regulated, suggesting that *sicily* mutants may contain misfolded mitochondrial proteins.

Sicily interacts with the preproteins of ND42 and NDUFS3 before their mitochondrial import

To study the function of Sicily, we performed a yeast two-hybrid screen and identified ND42, a CI subunit, as a Sicily interactor (Fig. 3 a). We confirmed this interaction by coimmunoprecipitation (IP; co-IP; Fig. 3 b). In these co-IP assays, we noticed that both Sicily and ND42 display two isoforms (Fig. 3 b, large [l] vs. small [s]). However, based on annotations, neither Sicily nor ND42 has more than one translational variant in *Drosophila*, suggesting that the isoforms are caused by posttranslational modifications. As NMTSs are cleaved from preproteins after mitochondrial import (Marc et al., 2002), we hypothesized that the two isoforms correspond to the uncleaved preproteins in cytoplasm and cleaved proteins in mitochondria, respectively. Indeed, the predicted length of the NMTS in Sicily is 11 aa (1.2 kD) and the NMTS of ND42 is 47 aa (5.1 kD), in agreement with the difference between the two isoforms.

To further test this hypothesis, we separated the cytoplasmic and mitochondrial fractions and found that the larger isoforms of both Sicily and ND42 are enriched in cytoplasm, whereas the smaller isoforms are enriched in mitochondria (Fig. 3 c). We then purified both isoforms of ND42 and subjected them to mass spectrometry analysis and identified five readings of peptide aa 16–37 from the larger isoform but none from the smaller isoform of ND42 (Fig. 3 d). As this peptide (aa 16–37) is derived from the predicted NMTS (aa 1–47), these

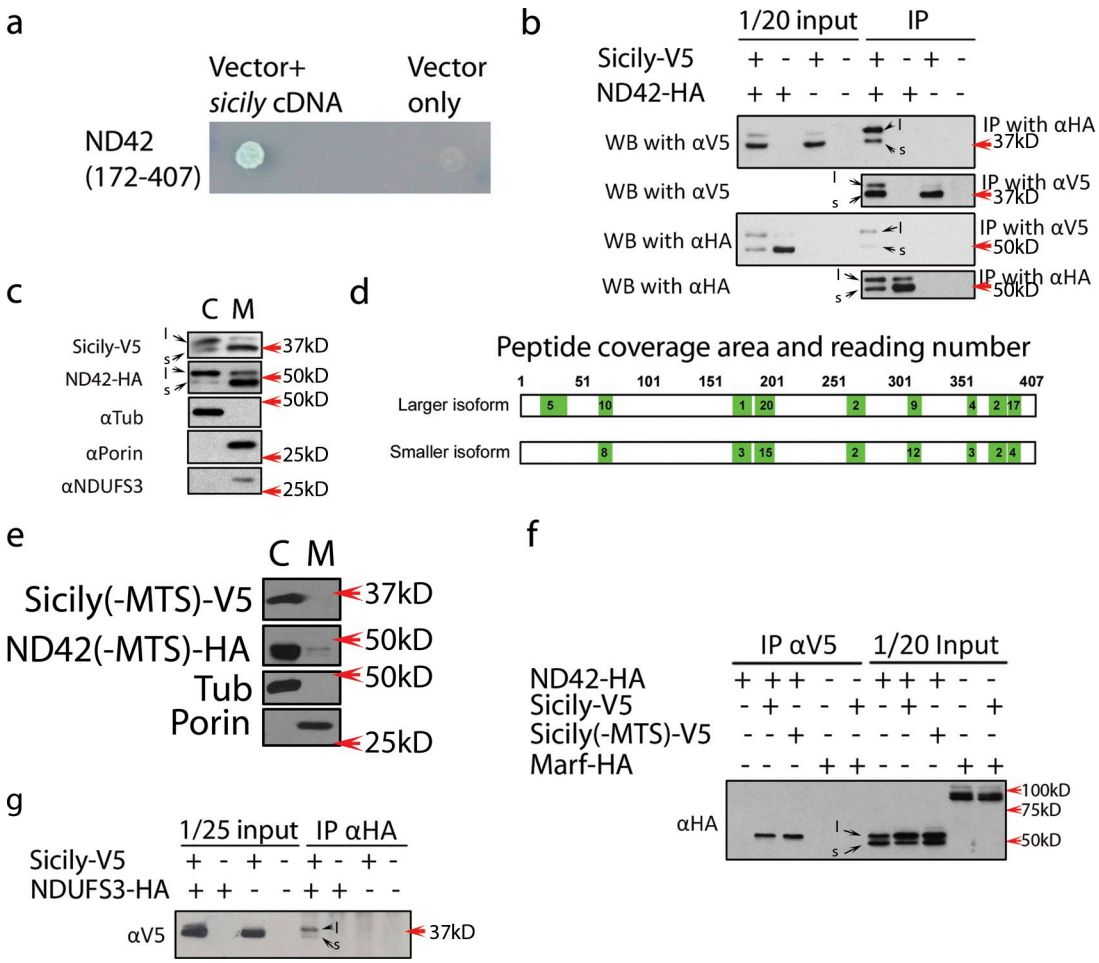

Figure 3. **Sicily interacts with CI subunits in cytoplasm.** (a) Sicily interacts with ND42 in a yeast two-hybrid assay. Yeast transfected with DNA are plated on SD-Trp-Leu-His media supplemented with X-α-gal. (b) Sicily and ND42 co-IP. S2 cells transfected with *Ubi-GAL4*, *UAS-Sicily-V5*, and/or *UAS-ND42-HA* were harvested and lysed 48 h after transfection. Both Sicily and ND42 exhibit two isoforms. The smaller isoforms (s) are more predominant in the input and IP, but the larger ones (l) are more predominant in the co-IP. (c) Immunoblots of subcellular fractionations of S2 cells expressing Sicily-V5 and ND42-HA. The larger isoforms of both Sicily and ND42 are enriched in cytoplasm (C), whereas the smaller isoforms are enriched in mitochondria (M). (d) Number of peptides of ND42 identified in mass spectrometry analysis. A peptide located within the predicted MTS of ND42 is identified in the larger, but not smaller, isoform. The area under curve (AUC) ratio of smaller isoform/larger isoform: 7% for the first peptide from the N terminus (aa 16–37); ~50% for the other peptides. (e) Immunoblots of subcellular fractionations of S2 cells expressing Sicily(-MTS)-V5 and ND42(-MTS)-HA. Both proteins are enriched in cytoplasm. (f) Co-IP of Sicily-MTS and ND42. Sicily-MTS shows similar binding affinity to ND42 as Sicily containing its MTS. An unrelated protein, Marf (fly homologue of Mitofusin), serves as a negative control. (g) Co-IP of Sicily and NDUFS3. Full-length Sicily preferentially interacts with NDUFS3. Tub, Tubulin; WB, Western blot.

data indicate that the NMTS is present in the larger isoform. We also repeat this experiment with Sicily. However, we were unable to obtain enough protein for mass spectrometry analysis.

In our co-IP assays, we also observed that the larger isoforms of Sicily and ND42 preferentially coprecipitate with each other (Fig. 3 b). This is not because of a generic bias of the IP, as most of the precipitated proteins consist of the smaller isoforms (Fig. 3 b, second and fourth boxes). These data indicate that the preproteins of Sicily and ND42 interact with each other in the cytoplasm, before their mitochondrial import.

To provide additional evidence that Sicily is able to interact with ND42 outside mitochondria, we engineered a Sicily protein lacking its predicted NMTS (aa 1–11), which we will refer to as Sicily-MTS. Sicily-MTS is mostly localized to cytoplasm (Figs. 3, e compare with c; and S3) and exhibits a similar binding affinity to ND42 as full-length Sicily (Fig. 3 f). To test whether Sicily-MTS rescues the phenotypes caused by loss of Sicily, we expressed Sicily-MTS in *sicily* mutants. Ubiquitous expression of Sicily-MTS, driven by *da-GAL4*, rescues the lethality, CI defects (Fig. 4, a and b), and decreased aconitase activity (Fig. 4 c) in *sicily* mutants. Together, these data indicate that the cytoplasmic role of Sicily is essential for CI function and that there is a dramatic rescue when compared with Fig. 1 d′. However, rescued animals display some subtle defects: a partial loss of "off" transient in their ERGs (Fig. 4 d), enlarged mitochondria at day 1 (Fig. 4, e and f, arrowhead and box), and some loss of PRs at day 10 (Fig. 1 c).

If Sicily regulates CI solely through ND42, overexpression of ND42 in *sicily* mutants might rescue some of the defects. However, this is not the case, as overexpression of ND42 does not rescue the lethality or retinal degeneration in *sicily* mutants, nor does it restore the abundance of NDUFS3 (unpublished data), suggesting that Sicily may affect multiple CI subunits in addition to ND42. Indeed, we also observe that Sicily

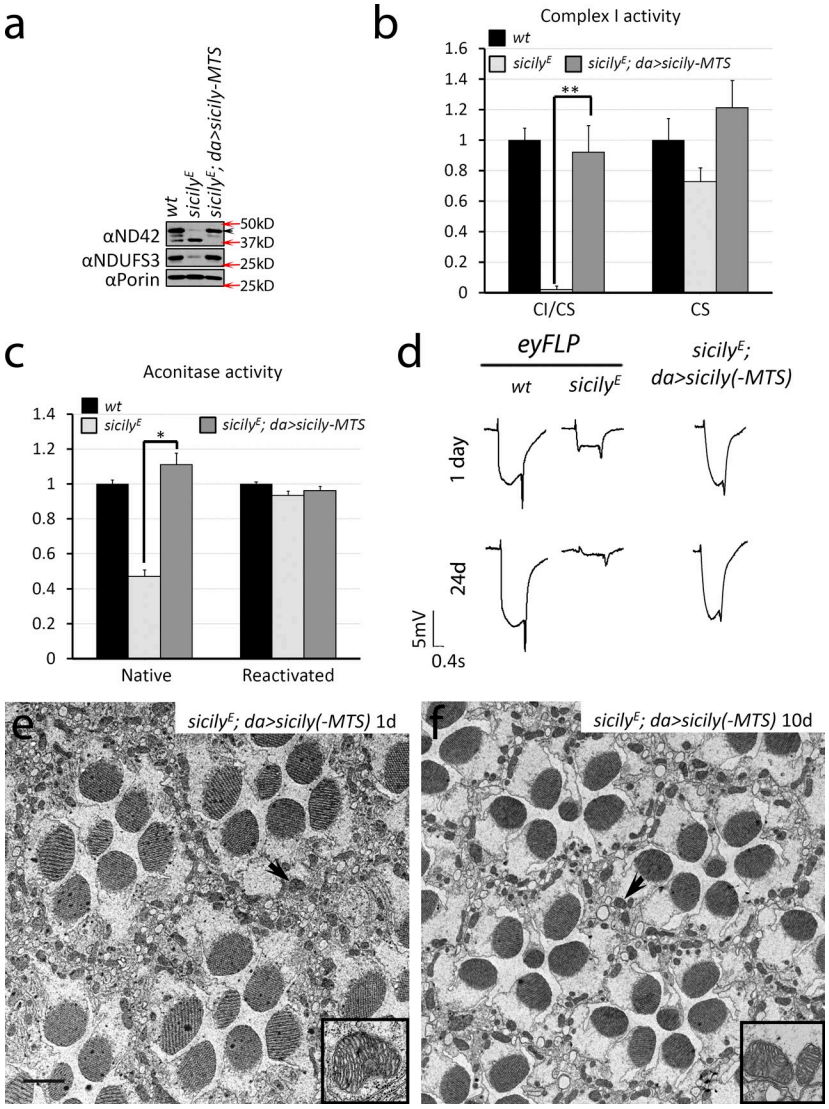

Figure 4. **Cytoplasmic Sicily (Sicily-MTS) rescues defects caused by loss of Sicily.** *sicily* mutant males that lack the protein express Sicily-MTS under the control of the *da-GAL4* driver, a ubiquitous driver. (a) These flies express wild-type levels of ND42 and NDUFS3 CI proteins. (b and c) Moreover, restoring the expression of *sicily* restores CI activity to wild-type levels (b) and reduces the elevated levels of ROS observed in *sicily* mutants, as it restores aconitase activity to wild-type levels (c). Data are presented as means ± SEM. (*, $P < 0.05$; **, $P < 0.01$; Student's *t* test). CS, citrate synthase. (d–f) In addition, we observe a partial rescue of the ERG defects (d) and retina morphology defects (e and f). Bar, 2 µm. The arrowheads indicate mitochondria that are also highlighted in the insets. The insets are 1 µm × 1 µm. *wild type* (*wt*) corresponds to y w *FRT19A* in a–d. The black arrow in a indicates the specific band.

interacts with NDUFS3 in co-IP assays and that the preprotein of Sicily again preferentially interacts (Fig. 3 g). Because NDUFS3 is a component that has been implicated in an early phase of CI assembly (Antonicka et al., 2003), it is likely that most CI subunits are affected when Sicily is lost.

Sicily is localized to cytoplasm and mitochondria in vivo

To determine where Sicily is localized in vivo when expressed at endogenous levels, we generated five antibodies. However, none recognized endogenous Sicily. We therefore tagged our genomic rescue construct with different tags: HA, V5, or mCherry. Unfortunately, the HA-tagged construct did not rescue the lethality. In addition, though the V5-tagged construct rescues the lethality and phenotypes, we were unable to detect the V5 epitope with either immunoblot or immunofluorescent staining in vivo, potentially because the endogenous level of Sicily is very low. The mCherry-tagged genomic rescue construct rescued the lethality and ERG defects of all alleles (unpublished data), showing that it is functional. Using a DsRed antibody (Takara Bio Inc.), we found that Sicily-mCherry is expressed in the ventral nerve cord (Fig. 5, a and b), larval brain (not depicted), motor neuron axons (Fig. 5, c and d), imaginal discs (Fig. 5, e and f), and muscles (not depicted). Hence, the gene is expressed in many tissues.

To determine whether Sicily is localized to cytoplasm and/or mitochondria in vivo, we costained Sicily-mCherry with two mitochondrial markers, ATP synthase (complex V [CV]) α subunit (Fig. 5; Baqri et al., 2009) and mitochondria-EYFP (not depicted; LaJeunesse et al., 2004). Sicily is only partially colocalized with these mitochondrial markers in all tissues observed, and a significant amount of protein is not colocalized but often juxtaposed to mitochondria. To confirm that Sicily is present in cytoplasm, we separated the mitochondrial and cytoplasmic fractions of *sicily* mutant flies rescued by genomically encoded Sicily-mCherry and immunoblotted them with the DsRed antibody. However, because of the low abundance of Sicily, we were unable to detect the endogenous protein on Western blot after fractionation (unpublished data). We therefore used an RFP nanobody (ChromoTek) to immunoprecipitate the Sicily-mCherry expressed by the genomic rescue construct (Fig. S3, c and d) in both fractions. These camel nanobodies have been

shown to be very efficient for IPs of tagged proteins (Fig. S3 c; Neumüller et al., 2012). As shown in Fig. S3 d, Sicily-mCherry is found in both fractions, showing that Sicily is present in both cytoplasm and mitochondria.

Sicily chaperones ND42 outside mitochondria

As the preproteins of Sicily and ND42 interact with each other, Sicily may stabilize the ND42 preprotein in cytoplasm and/or target it to mitochondria. If the latter hypothesis is correct, ND42 preprotein should accumulate in cytoplasm in *sicily* mutants. However, this is not observed (Fig. 6, a and b). Moreover, when overexpressed in *sicily* mutants, most ND42 is cleaved and localized to mitochondria (Fig. 6 b), further supporting that Sicily is not required to target ND42 to mitochondria. Hence, we propose that the cytoplasmic role of Sicily is to prevent the degradation of, rather than to target, ND42 preproteins to mitochondria.

To further test this hypothesis, we engineered an ND42 protein that lacks its NMTS (ND42-MTS) and coexpressed it with or without Sicily. We found that ND42-MTS is mostly localized to cytoplasm (Fig. 6, d–d′′ compared with c–c′′) and that coexpression of Sicily does not alter this localization (Figs. 6, e–f′′′; and 3 e), providing compelling evidence that Sicily does not target ND42 to mitochondria. On the other hand, coexpressing Sicily or Sicily-MTS leads to an increase of ND42-MTS levels (Fig. 6, e–g). These data strongly suggest that Sicily stabilizes ND42 and that it does not require its mitochondrial localization to perform this function. To confirm that Sicily stabilizes ND42 posttranslationally, we in vitro translated ND42 (full length) with or without Sicily and observed that ND42 is up-regulated when co-translating Sicily or Sicily-MTS (Fig. 6 h). These data show that Sicily prevents the degradation of ND42 preproteins.

As ND42 is down-regulated in the absence of Sicily, we next explored how ND42 is degraded in cytoplasm. We treated cells expressing ND42-MTS with a proteasome inhibitor, MG132, or a lysosomal inhibitor, bafilomycin A1, and found that ubiquitinated ND42-MTS is up-regulated when the proteasomal, but not the lysosomal, function is blocked (Fig. 6 i). These data suggest that the cytoplasmic ND42 is degraded mainly through the ubiquitin–proteasomal pathway. In summary, our data indicate that Sicily interacts with and stabilizes the preproteins of ND42 in cytoplasm.

Akin to Sicily, loss of ND42 causes CI defects and neurodegeneration

ND42 is an integral membrane protein of eukaryotic evolutionary origin, as it is not found in prokaryotes. Its human homologue, *NDUFA10*, has been found to be mutated in a case of Leigh syndrome with a CI deficiency (Hoefs et al., 2011). To probe the role of *ND42* in CI function and neurodegeneration, we knocked down *ND42* using two *UAS-RNAi* lines and showed that both RNAi lines lead to a severe knockdown of the protein (Fig. 7 a). The loss of ND42 also leads to the loss of NDUFS3 (Fig. 7 a) and reduced CI activity (Fig. 7 b), indicating that ND42 is an essential subunit of CI. Furthermore, larvae expressing the *ND42* RNAi also exhibited evidence of elevated ROS (Fig. 7 c) and an up-regulation of Hsp60 (Fig. 7 a), similar to loss of *sicily*. Finally, knockdown of ND42 in the visual system causes a severe retinal degeneration, as observed in *sicily* mutants (Figs. 7, d–e′′; and S4). In summary, loss of ND42, a CI subunit, and loss of Sicily lead to very similar biochemical and morphological defects.

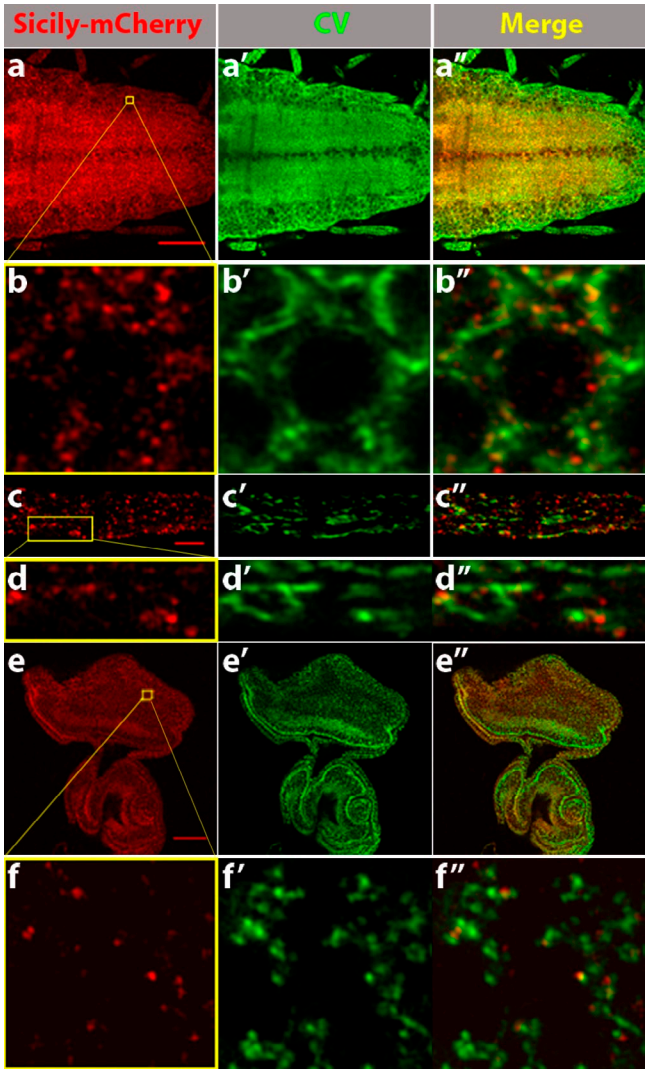

Figure 5. **Sicily is present in both cytoplasm and mitochondria.** (a–a′′) Third instar posterior ventral nerve cord of *sicily* mutants rescued with a genomic Sicily-mCherry construct costained with anti-DsRed (a) and anti-ATP synthase α subunit (complex V [CV]), a mitochondrial marker (a′). Merged in a′′. In b–b′′ are insets from a–a′′. (c–c′′) Motor neuron axons of third instar larvae. In d–d′′ are insets from c–c′′. (e–e′′) Eye imaginal disc. In f–f′′ are insets from e–e′′. Sicily is only partially colocalized with and often juxtaposed to CV staining. Bars: (a and e) 50 µm; (c) 5 µm.

Hsp90 interacts with Sicily to chaperone ND42

Because our data indicate that Sicily interacts with and stabilizes CI preproteins in the cytoplasm, we reasoned that it may act as a chaperone. As Sicily does not show homology to known chaperones, it may stabilize ND42 by recruiting other chaperones as a cofactor. To determine whether any cytosolic chaperones interact with Sicily, we performed in vivo co-IPs of Sicily-mCherry from whole flies using the RFP nanobody (Neumüller et al., 2012)

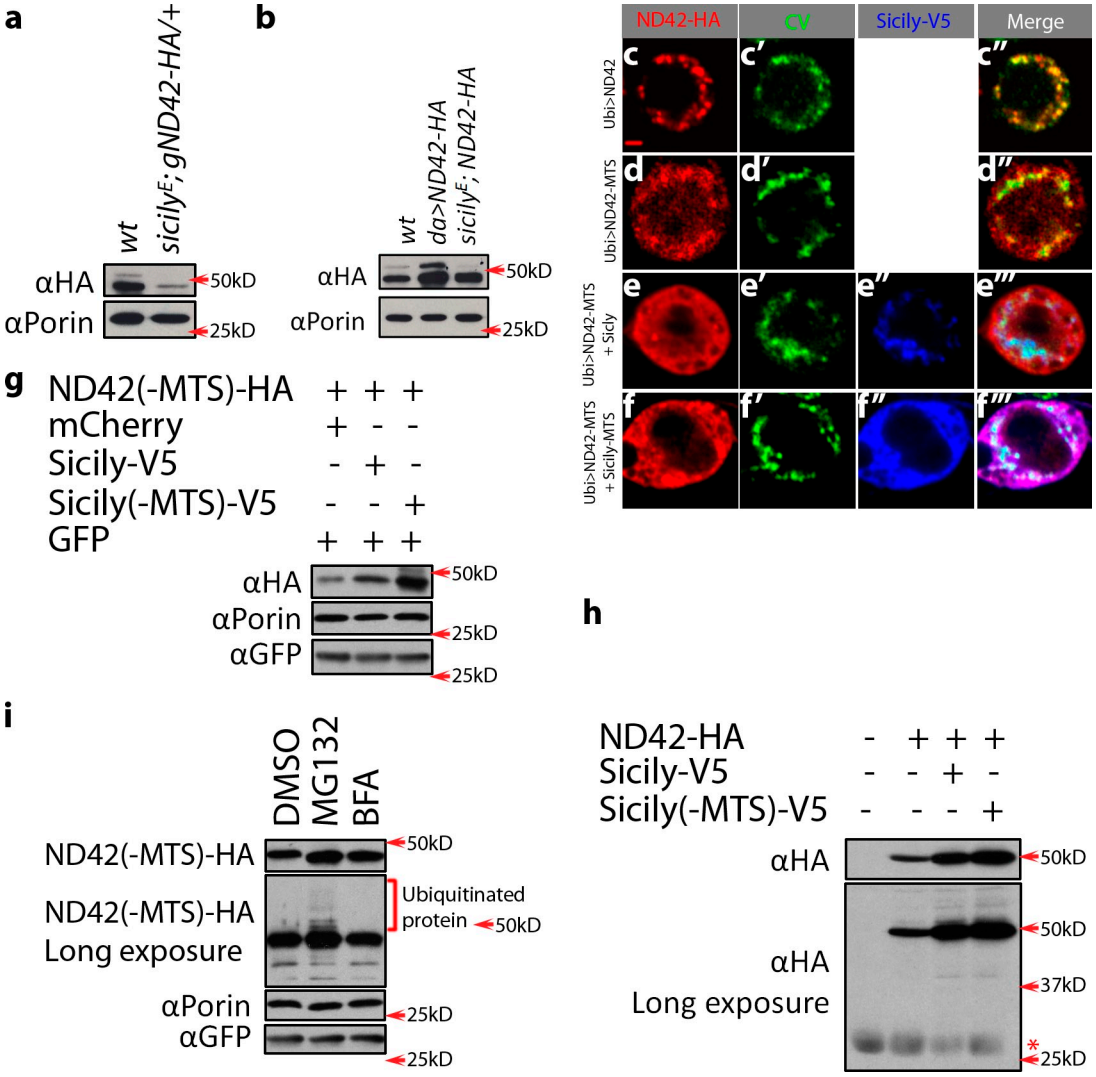

Figure 6. **Sicily stabilizes ND42 in cytoplasm.** (a) Immunoblots of whole body extract from *sicily* mutants expressing ND42-HA with a genomic construct. The overall level, including the level of ND42-HA preprotein, is down-regulated in *sicily* mutants, when compared with wild-type animals, suggesting that uncleaved/unprocessed ND42 does not accumulate in cytoplasm. *wild type* (*wt*) corresponds to *FRT19A; gND42-HA/+*. (b) Immunoblots of overexpressed ND42-HA in *sicily* mutants. The *da* refers to a *da-GAL4* driver that activates the UAS-ND42-HA construct ubiquitously at low levels. The level of mitochondrial ND42-HA is restored in *sicily* mutants, suggesting that Sicily is not required to target ND42 to mitochondria. However, the level of ND42 is reduced when Sicily is lost. *wild type* corresponds to *FRT19A; gND42-HA/gND42-HA*. (c–f′′) Effect of Sicily coexpression on cytoplasmic ND42. S2 cells expressing UAS-ND42-HA and/or UAS-Sicily-V5 under the control of *Ubi-GAL4*, a ubiquitously expressed driver, were costained with HA and CV antibodies. MTS-less ND42 (ND42-MTS) is more broadly localized (d–d′′) than full-length ND42 (c–c′′). Sicily (e–e′′′) or Sicily-MTS (f–f′′′), when coexpressed with ND42-MTS, do not target ND42-MTS to mitochondria but rather lead to an increase in the level of ND42-MTS (e–f′′′). These observations based on confocal microscopy are confirmed by Western blots in Fig. 6 g. (g) Coexpression of Sicily or Sicily-MTS leads to an increase of ND42-MTS level, when compared with coexpression of mCherry, an unrelated protein. Porin is used as a loading control, and GFP is used as a transfection control. (h) Immunoblots of in vitro translated ND42 either with or without co-translation of Sicily proteins. ND42 is up-regulated when Sicily or Sicily-MTS is co-translated. The asterisk points to a nonspecific protein that serves as a loading control. (i) Immunoblots of ND42-MTS in S2 cells treated with MG132, bafilomycin A1 (BFA), or a mock control, DMSO. MG132 treatment leads to ubiquitinated ND42. Bar, 2 µm.

followed by mass spectrometry analysis to identify interactors. We found several chaperones that interact with Sicily, including Hsp90 (CG1242). Hsp90 is a specialized chaperone that only functions at a late stage of substrate folding (Young et al., 2001). Specific cochaperones are required to stabilize its substrates, or these partially folded proteins are degraded (Johnson et al., 1998; Young et al., 2001). Hence, Sicily may be a cochaperone of Hsp90 to stabilize ND42. Indeed, Hsp90 binds to Sicily in an in vitro co-IP assay (Fig. 8 a), and Hsp90 coimmunoprecipitates ND42 only when Sicily is coexpressed (Fig. 8 b), indicating that Sicily, ND42, and Hsp90 are in a complex and that Sicily is required for Hsp90 to interact with ND42. To test whether ND42 facilitates the Hsp90–Sicily interaction, we compared co-IPs of Hsp90 and Sicily in the absence and presence of ND42 and found that the affinities are similar (Fig. 8 c), suggesting that ND42 does not affect the Hsp90–Sicily interaction. Together, these data indicate that Sicily is a primary binding partner of Hsp90, whereas ND42 is a secondary binding partner.

To confirm that the interaction between ND42 and Hsp90 occurs in cytoplasm through Sicily, we performed co-IPs and found that the coimmunoprecipitated ND42 is the isoform with the NMTS (Fig. 8 d), suggesting that cytoplasmic ND42 forms a

complex with Hsp90 and Sicily. To test whether Hsp90 directly or indirectly interacts with ND42, we cross-linked the complex with different cross-linkers (Fig. 8 d and not depicted). We observed that ND42 is present in cross-linked protein complexes (Fig. 8 d), whereas the level of native full-length ND42 is decreased (Fig. 8 d, third lane). In addition, less native full-length ND42 protein is immunoprecipitated when the proteins are cross-linked (Fig. 8 d, fifth and sixth lanes compared with fourth lane), suggesting that the ND42–Hsp90 interaction is not indirect. However, we were unable to detect ND42 in a cross-linked complex after IP (Fig. 8 d, sixth lane compared with third lane), suggesting that cross-linking eliminates their ability to be immunoprecipitated.

Hsp90 contains an ATPase domain that is required to stabilize its substrate. Inhibition of its ATPase activity by geldanamycin (GA), a drug that has been shown to be specific for Hsp90, leads to the proteasomal degradation of Hsp90 substrates and has been used to identify substrates for Hsp90 (Neckers, 2002, 2006; Weihofen et al., 2008; Okiyoneda et al., 2010). To determine whether the ATPase activity of Hsp90 is required for ND42 stability, we treated S2 cells expressing Sicily-V5 and ND42-HA with GA. As shown in Fig. 8 e, cells treated with GA exhibit a significant loss of ND42-HA as well as endogenous NDUFS3 (Fig. S5), whereas levels of unrelated proteins, Porin and a transfection control, GFP, are unaltered, indicating that Hsp90 activity is required for the stability of ND42 and NDUFS3. Interestingly, cells treated with GA also exhibit a loss of Sicily, suggesting that Sicily also requires Hsp90 for its stability, unlike canonical Hsp90 cochaperones or substrates.

To confirm that Hsp90 stabilizes Sicily and CI subunits in vivo, we analyzed protein levels of Sicily and CI in Hsp90 knockdown flies. As shown in Fig. 8 (f and g), flies expressing Hsp90 RNAi #1 exhibit severely decreased levels of Sicily, ND42, and NDUFS3 compared with controls. In addition, these flies are third instar lethal at 25°C and have extended larval stages, similar to *sicily* mutants. These data indicate that Hsp90 is also required for the abundance of Sicily and ND42 in vivo. In addition, flies expressing a weaker Hsp90 RNAi line #2 are viable but exhibit a less severe decrease in Sicily, ND42, and NDUFS3 levels upon aging (unpublished data). However, loss of ND42 does not negatively affect Sicily levels (Fig. 8 g), indicating that ND42 is not required for the stability of Sicily. This is consistent with the notion that ND42 is a secondary binding partner of the Sicily–Hsp90 complex (Fig. 8, b and c).

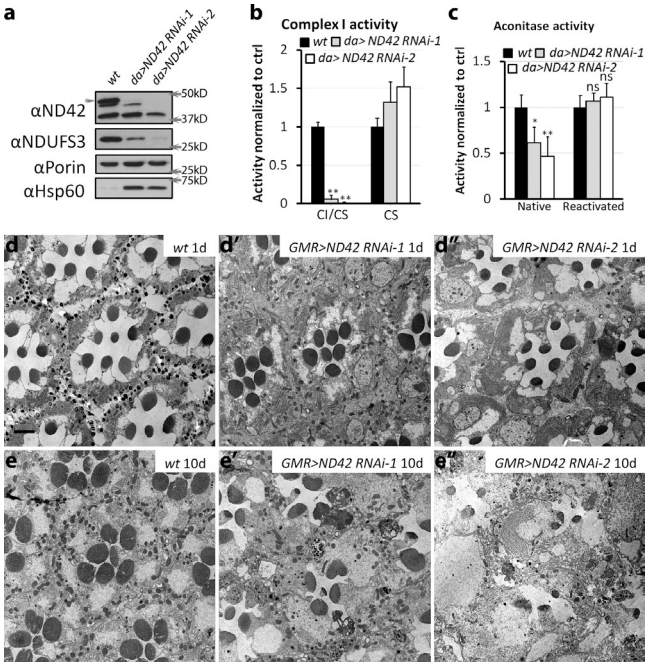

Figure 7. **Loss of ND42 phenocopies loss of Sicily.** (a) Immunoblots of CI subunits, Porin, and Hsp60 in mitochondrial fractions purified from third instar larvae expressing *ND42* RNAi. CI subunits are almost completely lost, and Hsp60 is up-regulated. The arrowhead indicates the specific band for ND42. (b) CI activity assay. Both RNAi-treated lines exhibit a near complete loss of CI activity. (c) Aconitase assay. Data are presented as means ± SEM (*, P < 0.05; **, P < 0.01; Student's *t* test; *n* = 3). (d–e'') TEM analysis of the retinas. Newly eclosed flies with *ND42* RNAi, driven by *GMR-GAL4*, display a normal number and arrangement of rhabdomeres (d' and d''), but the pigment cells are expanded when compared with the control flies (d). Upon aging for 10 d, the retinas of these flies degenerate (e' and e''), rhabdomeres are missing or dissociating, and the cell bodies of some PRs are vacuolated. Bar, 2 µm. (a–c) *wild type* (*wt*): *da/+*. (d and e) *wild type*: *GMR/+*. ctrl, control.

Discussion

Mitochondrial proteins with IMTSs are chaperoned by Hsp70 and Hsp90 in cytoplasm (Young et al., 2003; Fan et al., 2006). However, it is unknown how preproteins with NMTSs of eukaryotic origin in the nucleus are chaperoned. Here, we report that Sicily, the fly homologue of C8ORF38, plays a critical role in chaperoning these preproteins. Newly synthesized CI subunits bind Sicily that in turn recruits Hsp90 in the cytoplasm. In the absence of Sicily or Hsp90, at least two CI subunits are down-regulated, and CI activity is severely affected. These two subunits are recruited in the early (NDUFS3) and late (ND42) stages of CI assembly. In addition, a subunit encoded in the mitochondrial genome and translated in the matrix, ND1, is down-regulated in cells that lack C8ORF38 (McKenzie et al., 2011; Zurita Rendón and Shoubridge, 2012), suggesting that Sicily/C8ORF38 may chaperone CI proteins and preproteins in both cytoplasm and mitochondrial matrix. Alternatively, the lack of chaperoning CI preproteins in cytoplasm leads to a misassembled CI, which in turn causes the degradation of CI subunits translated in the matrix. These data are also consistent with the observation that unlike other CI assembly factors, neither Sicily (unpublished data) nor C8ORF38 interacts with CI intermediate subcomplexes in the matrix (Vogel et al., 2005; Saada et al., 2009; McKenzie et al., 2011). Hence, Sicily and C8ORF38 do not seem to function as classical assembly factors.

Hsp90 substrates typically are kinases, membrane receptors, and transcription factors (Young et al., 2001). However, Sicily does not belong to these classes of proteins. Furthermore, unlike canonical substrates, Sicily functions as a cochaperone for CI subunits. Hence, we propose that Sicily is a noncanonical substrate of Hsp90, which selectively binds and stabilizes secondary substrates, such as ND42 and NDUFS3. Recently, Zhao et al. (2005) and Zhao and Houry (2007) identified 22 novel Hsp90 interactors with similar properties in *Saccharomyces cerevisiae*.

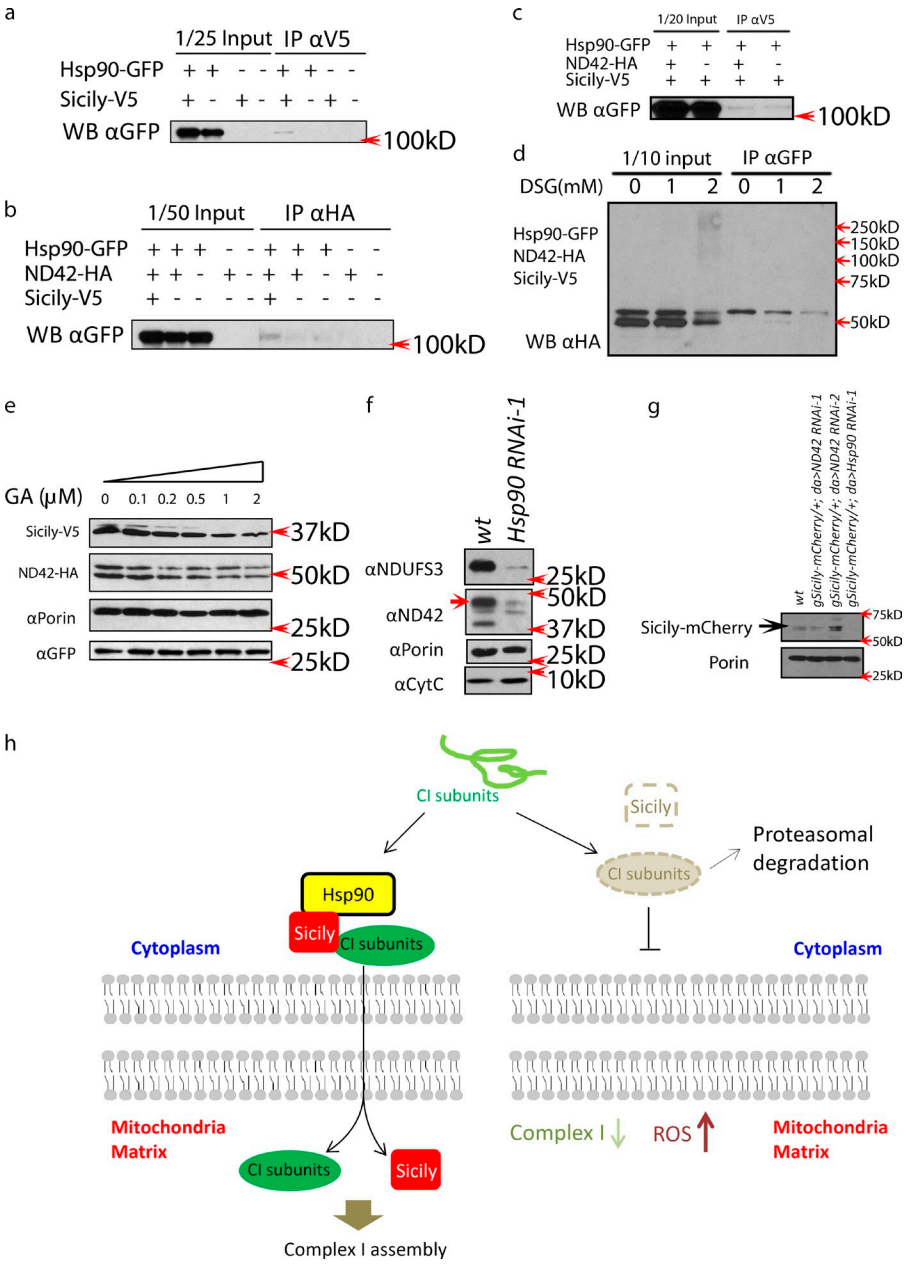

Figure 8. **Hsp90 is required for Sicily to chaperone ND42.** (a) Co-IP of Hsp90 and Sicily. (b) Co-IP of Hsp90 and ND42. Hsp90 interacts with ND42 only when Sicily is co-expressed. (c) Comparing co-IP of Hsp90 and Sicily in the presence or absence of ND42. ND42 does not affect Hsp90-Sicily binding. (d) Co-IP of Hsp90 and ND42 in the presence of cross-linkers. DSG, disuccinimidyl glutarate. (e) The effect of geldanamycin (GA), a specific inhibitor for Hsp90, on Sicily and ND42. The level of Sicily and ND42 are decreased when Hsp90 activity is inhibited. In flies, the typical active concentration of GA is in the 0.1–5-μM range (Auluck et al., 2005; Kampmueller and Miller, 2005). We used 0.1–2 μM. (f) CI proteins are down-regulated in flies expressing *Hsp90* RNAi. *wild type* (*wt*): *da/+*. (g) Endogenous Sicily is down-regulated in flies expressing *Hsp90*, but not *ND42*, RNAi. The arrowhead on the left indicates the specific band. *wild type*: *gSicily-mCherry/+; da/+*. (h) Working model: Sicily interacts with Hsp90 to chaperone some CI subunits, including ND42 and NDUFS3, in the cytoplasm. (left) Once imported, these subunits are incorporated into CI. (right) Loss of Sicily leads to the proteasomal degradation of CI subunits in the cytoplasm, loss of CI activity, and increased oxidative stress. WB, Western blot.

There are some interesting parallels between Sicily and Pink1, a protein involved in clearance of defective mitochondria. It has an NMTS and functions in cytoplasm, and its loss leads to ETC deficits and neurodegeneration (Clark et al., 2006; Dodson and Guo, 2007; Poole et al., 2008; Jin et al., 2010). Interestingly, Pink1 also interacts with cytosolic Hsp90 but rather as a substrate (Moriwaki et al., 2008) instead of as a cochaperone.

Leigh syndrome (subacute necrotizing encephalopathy) is an early onset, progressive, and fatal neurodegenerative disease. The classical presentation is characterized by onset in infancy/early childhood with rapid, progressive neurological decline and focal, bilateral lesions in the central nervous system. It is a mitochondrial disorder with extensive genetic heterogeneity, involving many genes in energy metabolism. Mutations in subunits and/or assembly factors for each of the mitochondrial ETC complexes have been shown to cause Leigh syndrome (Morris et al., 1996; Martín et al., 2005; Hoefs et al., 2011). CI deficiency is one of the most common causes of Leigh syndrome (Morris et al., 1996), and mutations in both *C8ORF38* (*sicily*) and *NDUFA10* (*ND42*) have been associated with the disease (Pagliarini et al., 2008; Hoefs et al., 2011). The phenotypes observed in the *Drosophila sicily* and *ND42* mutants are similar to defects observed in Leigh syndrome patients and include progressive dysfunction and deterioration of neurons, ETC deficiency, and increased steady-state levels of ROS (Nunnari and Suomalainen, 2012). In addition, mutations that affect complex II in flies and cause Leigh syndrome in patients also cause very similar phenotypes (Mast et al., 2008). These similarities indicate that the molecular mechanisms presented here are relevant to our understanding of the molecular pathophysiology of Leigh syndrome.

Materials and methods

Screen and mapping

To identify novel genes on the *Drosophila* X chromosome that cause a neurodegenerative phenotype, we performed a large forward genetic screen. In the screen, isogenized *y w P{neoFRT}19A* males were treated with 7.5–15 mM ethyl methane sulfonate and crossed to *Df(1)JA27/FM7c, Kr-Gal4, UAS-GFP* virgins. The *y w *mut FRT19A/FM7c, Kr-Gal4, UAS-GFP* offspring were crossed to *FM7c, Kr-Gal4, UAS-GFP/Y* males to generate stocks. Stocks that did not produce *y w *mut FRT19A* males were retained, as they carry mutations in essential genes on the X chromosome. Out of 33,887 stocks, 5,859 lethal mutants were identified.

For ERG recording, *y w *mut (lethal) FRT19A/FM7c, Kr-Gal4, UAS-GFP* flies were crossed to *y w P{w+} cl(1) FRT19A/Dp(1;Y)y+; eyFLP* to generate flies with mutant clones in the eyes, and ERGs were performed as previously described (Verstreken et al., 2003; Ly et al., 2008). Flies were immobilized on glass slides. A reference glass electrode was inserted in the fly thorax, and a recording electrode was placed on the surface of the fly eye. Both electrodes were filled with 100 mM NaCl. Light flashes of 1 s were delivered using a halogen lamp. We recorded ERGs from ∼3,100 stocks. We were unable to assay all mutants, as some block eclosion, cause cell lethality or eye roughness, or produce clones that are too small to record from. We recorded from young (1–3 d old) and aged (24 d old) flies and identified 770 mutants with ERG defects.

For mapping and complementation tests, *y w *mut (lethal) FRT19A/FM7c, Kr-Gal4, UAS-GFP* females were crossed to males from 10 large 1;Y duplications (from Bloomington Drosophila Stock Center duplication kit 1), genotype *Df(1)/Dp(1;Y)/C(1)DX*, which together cover 50% of the X chromosome (Cook et al., 2010; Venken et al., 2010). Rescued *y w *mut (lethal) FRT19A/Dp(1;Y)* males were backcrossed to virgins from the same duplication stock by which they were rescued to generate stocks. Mutants rescued by the same duplications were subjected to complementation tests. All *XE07* alleles were rescued by *Dp(1;Y)BSC1*, and males carrying *XE07* alleles were crossed to deficiencies within the *Dp(1;Y)BSC1* region, including *Df(1)BSC726* and *Df(1)BSC543* (Parks et al., 2004; Ryder et al., 2004; Thibault et al., 2004). The *P* element insertion line affecting *CG15738*, *yw P{w[+mC], y[+mDint2]=EPgy2}CG15738[EY02706]/FM7c*, was generated by the Gene Disruption Project (Bellen et al., 2004).

Drosophila stocks and crosses

For RNAi experiments, *ND42* RNAi#1, *yv; P{TRiP.HM05104}attP2* (Ni et al., 2009); *ND42* RNAi#2, *w; P{GD6220}v14444*, (Dietzl et al., 2007); and *Hsp90* RNAi#1, *y sc v; P{TRiP.HMS00899}attP2*, and #2, *y sc v; P{TRiP.HMS00796}attP2* (Ni et al., 2009), were crossed to *da-GAL4*.

Molecular cloning

For the *sicily* genomic rescue construct, a DNA fragment containing *Drosophila* X:11783223…11788796 was retrieved from bacterial artificial chromosome clone BACR19M14 (Osoegawa et al., 2001; Osoegawa and de Jong, 2004) and subcloned into p[w+]attB (Koch et al., 2009) using BamHI and NotI sites. The tags added are 3×HA, V5, and mCherry (Shaner et al., 2004).

For *ND42* genomic rescue construct, a DNA fragment containing *Drosophila* 3R:17852760…17855427 was retrieved from BAC clone BACR24J06 (Osoegawa et al., 2001; Osoegawa and de Jong, 2004) and subcloned into p[w+]attB (Koch et al., 2009) using BglII and NotI sites. The tags were added by chimeric PCR.

For cDNA constructs, the coding sequence of *sicily*, *ND42*, or *Hsp90* was retrieved from cDNA clones RE44923, LD29280, or AT20544 (Rubin et al., 2000; Stapleton et al., 2002), respectively, and subcloned into pUASattB (Bischof et al., 2007) vector using KpnI (for *sicily*) or EcoRI and NotI (for *ND42* and *Hsp90*) sites. Kozak consensus sequences, AAAs, were added to the 5′ of the CDSs. Tags were added by either chimeric PCR or included in the primers. The MTSs of Sicily and ND42 are predicted using Mitoprot (Claros and Vincens, 1996). For pUASattB-Sicily-MTS and pUASattB-ND42-MTS constructs, the predicted MTSs, aa 1–11 for Sicily and aa 1–47 for ND42, are truncated. For the human *C8orf38* cDNA construct, the CDS of human *C8orf38* was retrieved from cDNA clone 5245422 from the Mammalian Gene Collection (Strausberg et al., 2002) and subcloned into pUASattB vector using EcoRI and NotI sites. A Kozak consensus sequence, AAA, was added to the 5′ of the CDS.

Transgenic flies

Transgenic flies containing genomic or cDNA constructs were generated by injecting certain plasmids into the embryos of *y w;; PBac{y[+]-attP}VK00033* (chromosome III) and *y w; PBac{y[+]-attP}VK00037* (chromosome II; Venken et al., 2006).

Immunofluorescent staining

For tissue staining, the rabbit anti-DsRed antibody (Takara Bio Inc.) was extensively preabsorbed against tissues from *sicilyE;;gSicily* larvae before use. The antibodies were used at the following concentrations: DsRed, 1:200, and mouse anti-ATP synthase α subunit (CV; MitoSciences), 1:500. For S2 cell staining, the following antibodies were used: rat anti-HA (Roche), mouse anti-V5 (Invitrogen), rabbit anti-V5 (GenScript), and mouse anti-CV (MitoSciences). All primary antibodies were used at 1:100. Secondary antibodies conjugated to Cy3 (Jackson ImmunoResearch Laboratories, Inc.) or Alexa Fluor 488 (Invitrogen) were used at 1:250. Samples were mounted in Vectashield (Vector Laboratories) before being analyzed under a confocal microscope.

All our confocal scans were acquired with a confocal microscope (model LSM510; Carl Zeiss) with its accompanying software using Plan Apochromat 40×, NA 1.4 and Plan Apochromat 63×, NA 1.4 objectives (Carl Zeiss) at room temperature. Images were captured by a camera (AxioCam HRc; Carl Zeiss). Images are processed using ImageJ (National Institutes of Health). Deconvolution was performed using the Tikhonov–Miller method.

TEM

TEM was performed similarly as previously described (Zhai et al., 2006). Adult heads were dissected and fixed in cacodylate buffer containing 4% paraformaldehyde/2% glutaraldehyde and postfixed in 1% OsO_4. Fixed samples were dehydrated in ethanol and embedded in EMBED-812 resin (Electron Microscopy Sciences). Plastic sections were stained with 4% uranyl acetate followed by lead citrate before examination with an electron microscope (1010; JEOL).

Quantitative PCR

Drosophila whole DNA (genomic and mitochondrial) was purified from control or *sicily* mutant larvae as the template for PCR. The template DNA was mixed with primers and green supermix reagent (iQ SYBR; Bio-Rad Laboratories). PCR was performed in a thermal cycler (iCycler; Bio-Rad Laboratories), and the data were collected and analyzed using the optical module (iQ5; Bio-Rad Laboratories) and related software following the manufacturer's instructions.

The following primer pairs were used to amplify a genomic DNA fragment corresponding to *CG9277/β-Tubulin* or a mitochondrial DNA fragment corresponding to *CG34083/ND5*, respectively: *β-Tubulin* forward, 5′-CCTTCCCACGTCTTCACTTC-3′; and *β-Tubulin* reverse, 5′-TTCTTGGCATCGAACATCTG-3′; and *ND5* forward, 5′-GCAGAAACAGGTGTAGGAGCA-3′; and *ND5* reverse, 5′-GCTGCTATAACTAAAAGAGCTCAGA-3′.

Yeast two-hybrid screen

The yeast two-hybrid screen was performed using the Matchmaker kit following the manufacturer's instructions (Takara Bio Inc.). Sicily (aa 47–334) was subcloned into the pGBK-T7 vector as the bait. The library DNA for prey was a collection of fly embryo cDNAs cloned into pACT2 vector. AH109 cells were transformed with both bait and prey constructs and plated on synthetic defined (SD) Trp-Leu media with X-α-gal. Blue colonies were further tested on SD-Trp-Leu-His media supplemented with X-α-gal. Viable and blue colonies were selected for plasmid sequencing.

Mitochondria isolation, subcellular fractionation, and enzymatic activity assays

Mitochondria were extracted as previously described (Graham et al., 2010). Flies are homogenized in extraction buffer (5 mM Hepes, pH 7.5, 210 mM mannitol, 70 mM sucrose, and 1 mM EGTA), and the lysate was subjected to centrifuge at 3,000 *g* for 10 min. The supernatant was then subjected to centrifuge at 8,000 *g* for 20 min. The supernatant contains the cytoplasmic fraction, whereas the pellet contains mitochondria.

For enzymatic assays, purified mitochondria were resuspended in ETC assay buffer (250 mM sucrose, 2 mM EDTA, and 100 mM Tris-HCl, pH 7.4), or aconitase assay buffer (1 mM L-cysteine, 50 mM Tris, 30 mM sodium citrate, and 0.5 mM $MnCl_2$, pH 7.3). Mitochondrial membranes were broken by sonication (4× 5-s pulse and 60% power) using an ultrasonic cell disruptor (Microson XL-2000; Misonix). Enzymatic activity assays were performed as previously described (Emptage et al., 1983; Das et al., 2001; Graham et al., 2010). CI activity (NADH/ubiquinone oxidoreductase) was determined by measuring oxidation of NADH at 340 nm (using ferricyanide as the electron acceptor) in a reaction mixture of 25 mm potassium phosphate, pH 7.5, 0.2 mm NADH, and 1.7 mm potassium ferricyanide. Complex II activity (succinate dehydrogenase) was determined by measuring the reduction of the artificial electron acceptor 2,6-dichlorophenol-indophenol at 600 nm in a reaction mixture of 25 mm potassium phosphate, pH 7.5, 20 mm succinate, 0.5 mm 2,6-dichlorophenol-indophenol, 10 µm rotenone, 2 µg/ml antimycin A, and 2 mm potassium cyanide.

Complex III activity (ubiquinol/cytochrome *c* oxidoreductase) was determined by measuring the reduction of cytochrome *c* at 550 nm in a reaction mixture of 25 mm potassium phosphate, pH 7.5, 35 µm reduced decylubiquinone, 15 µm cytochrome *c*, 10 µm rotenone, and 2 mm potassium cyanide. Complex IV activity (cytochrome *c* oxidase) was determined by measuring the oxidation of cytochrome *c* at 550 nm in a reaction mixture of 10 mm potassium phosphate, pH 7.5, and 0.1 mm reduced cytochrome *c*. Citrate synthase activity was determined by measuring the reduction of 5,5′-dithiobis(2-nitrobenzoic acid) at 412 nm, which is coupled to the reduction of acetyl–coenzyme A by citrate synthase in the presence of oxaloacetate. The reaction mixture consists of 10 mm potassium phosphate, pH 7.5, 100 µm 5,5′-dithiobis(2-nitrobenzoic acid), 50 µm acetyl–coenzyme A, and 250 µm oxaloacetate. All activities were calculated as nanomoles/minute/milligram of protein, normalized to citrate synthase activity.

For native aconitase activity, the conversion of citrate into α-ketoglutarate was monitored at 340 nm with a 96-well plate based on the coupled reduction of NADP to NADPH under isocitrate dehydrogenase using a plate reader (Infinite M200; Tecan) at 30°C. Reduced aconitase activity was measured by incubation with 0.2 mM ferrous ammonium sulfate (Fluka) for 5 min in the reaction well before performing the enzymatic activity assay. All activities were calculated as nanomoles of NADPH/minute/milligram of total protein.

Protein extraction and immunoblot

Tissues or purified mitochondria were homogenized in Laemmli buffer supplemented with protease inhibitor cocktail (Complete; Roche) and heated at 98°C for 10 min. Antibodies were used at the following concentrations for immunoblots: rabbit anti-DsRed, 1:1,000; mouse anti-NDUFS3 (MitoSciences), 1:10,000; chicken anti-NDUFA10 (Abcam), 1:1,000; chicken anti-Porin (Graham et al., 2010), 1:10,000; mouse anti–cytochrome *d* (MitoSciences), 1:5,000; mouse anti-Hsp60 (LK-1; Abcam), 1:1,000; and mouse anti–β-Tubulin (E7; Developmental Studies Hybridoma Bank), 1:5,000. All secondary antibodies conjugated to HRP (Jackson ImmunoResearch Laboratories, Inc.) were used at 1:5,000.

Cell culture and IP

S2 cells were cultured under standard conditions. The transfections were performed using Lipofectamine LTX (Invitrogen) following the manufacturer's instructions. Proteins are expressed using the UAS/GAL4 system, driven by *Ubiquitin-63E–Gal4*. For immunofluorescent staining, cells were fixed 24 h after transfection. For protein analyses with SDS-PAGE and/or immunoblots, cells were harvested and lysed 48 h after transfection except for the ones treated with GA. Proteins were then extracted for different assays.

MG132 (Sigma-Aldrich) and bafilomycin A1 (Sigma-Aldrich) were dissolved in DMSO and added to cells with the final concentrations of 20 µM (MG132) and 100 nM (bafilomycin) 48 h after transfection. Cells were treated for 2 h. GA was dissolved in DMSO and added to cells with certain concentrations 24 h after transfection. Cells were treated with GA for 12 h.

For cross-linking experiments, dithiobis(succinimidyl propionate), disuccinimidyl glutarate, or disuccinimidyl suberate (Thermo Fisher Scientific) was dissolved in DMSO and added to cells with certain concentrations. Cells were harvested 48 h after transfection, resuspended in PBS, treated with the cross-linkers for half an hour, and quenched in 50 mM Tris, pH 7.4, for 15 min at room temperature. To identify the molecular difference between two isoforms of ND42 or Sicily, cells were resuspended in Laemmli buffer, proteins were separated by SDS-PAGE, and bands with specific molecular sizes were cut and subjected to mass spectrometry analysis.

Co-IP was performed as previously described (Tong et al., 2011). Cells were lysed in lysis buffer (50 mM Tris, pH 7.4, 150 mM NaCl, 1 mM EDTA, 1% NP-40, and protease inhibitor cocktail), and the soluble fractions were precleared using empty beads. Protein complexes were then immunoprecipitated using either mouse anti-HA–agarose (Sigma-Aldrich), goat anti-V5–agarose (Bethyl Laboratories, Inc.), or GFP-Trap A–coupled agarose beads (ChromoTek). The following antibodies were used for immunoblots: rat anti-HA, mouse anti-V5, rabbit anti-V5, chicken anti-GFP (Abcam), and rabbit anti-DsRed. All primary antibodies are used at 1:1,000.

For endogenous IP, 1 ml *sicily^{E} FRT19A;;gRes-mCherry* adult flies were homogenized in lysis buffer. IP was performed using RFP-Trap A–coupled agarose beads following the manufacturer's instructions. Precipitated proteins were separated by SDS-PAGE and subjected to Western blotting or mass spectrometry analysis.

In vitro translation

Sicily and ND42 cDNA were cloned into pET21(a) vectors. In vitro translation was performed using the quick coupled transcription/translation system (TNT; Promega) following the manufacturer's instructions.

Mass spectrometry

Protein samples were boiled with Laemmli buffer and subjected to SDS-PAGE (4–20% Tris/glycine gel [Novex; Invitrogen]). Coomassie brilliant blue–stained protein bands were excised and subjected to in-gel digestion with trypsin essentially as previously described (Jung et al., 2005). Nano-HPLC tandem mass spectrometry analysis of the isolated protein complex using advanced linear ion trap-mass spectrometer (LTQ Orbitrap Velos; Thermo Fisher Scientific) was performed as previously described (Jung et al., 2008). In brief, each tryptic peptide was loaded onto a 0.3 × 5–mm C18 trap column (Zorbax 300SB; Agilent Technologies) equilibrated in 0.1% formic acid in water and washed for 5 min, and then, the trap column was switched in line with an in-house 100-mm × 75-µm column packed with a C18 matrix (Jupiter 4 µm Proteo 90 Å; Phenomenex) equilibrated in 0.1% formic acid/water. The peptides were separated with a 50-min discontinuous gradient of acetonitrile/0.01% formic acid (5–60% acetonitrile for 20 min) at a flow rate of 200 nl/min. Separated peptides were directly electrosprayed into the mass spectrometer using nanospray source with a voltage of 2.5 kV applied to the liquid junction. The mass spectrometer was operated in the data-dependent mode acquiring fragmentation spectra of the top 20 strongest ions. Obtained tandem mass spectrometry spectra were searched against *Drosophila* RefSeq database from FlyBase (ftp://ftp.flybase.net/genomes/aaa/) with Mascot algorithm (Mascot 2.3; Matrix Science) embedded in Proteome Discoverer 1.2 interface (Thermo Fisher Scientific). The precursor mass tolerance was confined within 10 ppm with fragment mass tolerance of 0.5 D and a maximum of three missed cleavages allowed. Assigned peptides were filtered with 5% false discover rate and subjected to verifications to eliminate false identifications.

Statistical analysis

Two-tailed Student's *t* tests were applied to the data as indicated in the legends.

Online supplemental material

Fig. S1 shows the quantifications in the TEM of Fig. 1. Fig. S2 shows the mapping and lethal staging of Sicily (related to Fig. 2). Fig. S3 shows the localization of Sicily and Sicily-MTS (related to Figs. 3, 4, 5, and 6). Fig. S4 shows the quantification of the TEM of Fig. 7. Fig. S5 shows that Hsp90 is required to stabilize endogenous NDUFS3 (related to Fig. 8). Online supplemental material is available at http://www.jcb.org/cgi/content/full/jcb.201208033/DC1. Additional data are available in the JCB DataViewer at http://dx.doi.org/10.1083/jcb.201208033.dv.

We thank Adeel Jawaid, Yu-fei Chen, Clarissa Benitez, and Xiao Shi for their support in the ERG screen of X chromosome mutants. We thank Yuchun He and Hongling Pan for their injections to create transgenic flies. We thank Lita Duraine for her support in the TEM. We thank Patrik Verstreken and Karen Schulze for their comments. We are grateful to the Bloomington Stock Center and the Developmental Studies Hybridoma Bank for reagents. We thank the Transgenic RNAi Project at Harvard Medical School (National Institutes of Health/National Institute of General Medical Sciences R01-GM084947) for providing transgenic RNAi fly stocks used in this study. Confocal microscopy was supported by the Baylor College of Medicine Intellectual and Developmental Disabilities Research Center.

B. Xiong is supported by The Houston Laboratory and Population Sciences Training Program in Gene–Environment Interaction from the Burroughs Wellcome Fund. V. Bayat received support from the Edward and Josephine Hudson Scholarship Fund. S. Yamamoto was supported by a fellowship from the Nakajima Foundation. H.J. Bellen is an Investigator of the Howard Hughes Medical Institute.

Submitted: 7 August 2012
Accepted: 19 February 2013

References

Antonicka, H., I. Ogilvie, T. Taivassalo, R.P. Anitori, R.G. Haller, J. Vissing, N.G. Kennaway, and E.A. Shoubridge. 2003. Identification and characterization of a common set of complex I assembly intermediates in mitochondria from patients with complex I deficiency. *J. Biol. Chem.* 278:43081–43088. http://dx.doi.org/10.1074/jbc.M304998200

Auluck, P.K., M.C. Meulener, and N.M. Bonini. 2005. Mechanisms of suppression of alpha-synuclein neurotoxicity by geldanamycin in *Drosophila*. *J. Biol. Chem.* 280:2873–2878. http://dx.doi.org/10.1074/jbc.M412106200

Baqri, R.M., B.A. Turner, M.B. Rheuben, B.D. Hammond, L.S. Kaguni, and K.E. Miller. 2009. Disruption of mitochondrial DNA replication in

Drosophila increases mitochondrial fast axonal transport in vivo. *PLoS ONE*. 4:e7874. http://dx.doi.org/10.1371/journal.pone.0007874

Bayat, V., I. Thiffault, M. Jaiswal, M. Tétreault, T. Donti, F. Sasarman, G. Bernard, J. Demers-Lamarche, M.J. Dicaire, J. Mathieu, et al. 2012. Mutations in the mitochondrial methionyl-tRNA synthetase cause a neurodegenerative phenotype in flies and a recessive ataxia (ARSAL) in humans. *PLoS Biol.* 10:e1001288. http://dx.doi.org/10.1371/journal.pbio.1001288

Bellen, H.J., R.W. Levis, G. Liao, Y. He, J.W. Carlson, G. Tsang, M. Evans-Holm, P.R. Hiesinger, K.L. Schulze, G.M. Rubin, et al. 2004. The BDGP gene disruption project: single transposon insertions associated with 40% of *Drosophila* genes. *Genetics*. 167:761–781. http://dx.doi.org/10.1534/genetics.104.026427

Bischof, J., R.K. Maeda, M. Hediger, F. Karch, and K. Basler. 2007. An optimized transgenesis system for *Drosophila* using germ-line-specific phiC31 integrases. *Proc. Natl. Acad. Sci. USA*. 104:3312–3317. http://dx.doi.org/10.1073/pnas.0611511104

Brand, A.H., and N. Perrimon. 1993. Targeted gene expression as a means of altering cell fates and generating dominant phenotypes. *Development*. 118:401–415.

Brand, M.D. 2010. The sites and topology of mitochondrial superoxide production. *Exp. Gerontol.* 45:466–472. http://dx.doi.org/10.1016/j.exger.2010.01.003

Bratic, A., A. Wredenberg, S. Grönke, J.B. Stewart, A. Mourier, B. Ruzzenente, C. Kukat, R. Wibom, B. Habermann, L. Partridge, and N.G. Larsson. 2011. The bicoid stability factor controls polyadenylation and expression of specific mitochondrial mRNAs in *Drosophila melanogaster*. *PLoS Genet.* 7:e1002324. http://dx.doi.org/10.1371/journal.pgen.1002324

Carroll, J., I.M. Fearnley, J.M. Skehel, R.J. Shannon, J. Hirst, and J.E. Walker. 2006. Bovine complex I is a complex of 45 different subunits. *J. Biol. Chem.* 281:32724–32727. http://dx.doi.org/10.1074/jbc.M607135200

Clark, I.E., M.W. Dodson, C. Jiang, J.H. Cao, J.R. Huh, J.H. Seol, S.J. Yoo, B.A. Hay, and M. Guo. 2006. *Drosophila* pink1 is required for mitochondrial function and interacts genetically with parkin. *Nature*. 441:1162–1166. http://dx.doi.org/10.1038/nature04779

Claros, M.G., and P. Vincens. 1996. Computational method to predict mitochondrially imported proteins and their targeting sequences. *Eur. J. Biochem.* 241:779–786. http://dx.doi.org/10.1111/j.1432-1033.1996.00779.x

Cook, R.K., M.E. Deal, J.A. Deal, R.D. Garton, C.A. Brown, M.E. Ward, R.S. Andrade, E.P. Spana, T.C. Kaufman, and K.R. Cook. 2010. A new resource for characterizing X-linked genes in *Drosophila melanogaster*: systematic coverage and subdivision of the X chromosome with nested, Y-linked duplications. *Genetics*. 186:1095–1109. http://dx.doi.org/10.1534/genetics.110.123265

Das, N., R.L. Levine, W.C. Orr, and R.S. Sohal. 2001. Selectivity of protein oxidative damage during aging in *Drosophila melanogaster*. *Biochem. J.* 360:209–216. http://dx.doi.org/10.1042/0264-6021:3600209

de Souza-Pinto, N.C., D.M. Wilson III, T.V. Stevnsner, and V.A. Bohr. 2008. Mitochondrial DNA, base excision repair and neurodegeneration. *DNA Repair (Amst.)*. 7:1098–1109. http://dx.doi.org/10.1016/j.dnarep.2008.03.011

Dietzl, G., D. Chen, F. Schnorrer, K.C. Su, Y. Barinova, M. Fellner, B. Gasser, K. Kinsey, S. Oppel, S. Scheiblauer, et al. 2007. A genome-wide transgenic RNAi library for conditional gene inactivation in *Drosophila*. *Nature*. 448:151–156. http://dx.doi.org/10.1038/nature05954

Dodson, M.W., and M. Guo. 2007. Pink1, Parkin, DJ-1 and mitochondrial dysfunction in Parkinson's disease. *Curr. Opin. Neurobiol.* 17:331–337. http://dx.doi.org/10.1016/j.conb.2007.04.010

Emptage, M.H., J.L. Dreyers, M.C. Kennedy, and H. Beinert. 1983. Optical and EPR characterization of different species of active and inactive aconitase. *J. Biol. Chem.* 258:11106–11111.

Fan, A.C., M.K. Bhangoo, and J.C. Young. 2006. Hsp90 functions in the targeting and outer membrane translocation steps of Tom70-mediated mitochondrial import. *J. Biol. Chem.* 281:33313–33324. http://dx.doi.org/10.1074/jbc.M605250200

Garcia, M., X. Darzacq, T. Delaveau, L. Jourdren, R.H. Singer, and C. Jacq. 2007. Mitochondria-associated yeast mRNAs and the biogenesis of molecular complexes. *Mol. Biol. Cell*. 18:362–368. http://dx.doi.org/10.1091/mbc.E06-09-0827

Graham, B.H., Z. Li, E.P. Alesii, P. Versteken, C. Lee, J. Wang, and W.J. Craigen. 2010. Neurologic dysfunction and male infertility in *Drosophila* porin mutants: a new model for mitochondrial dysfunction and disease. *J. Biol. Chem.* 285:11143–11153. http://dx.doi.org/10.1074/jbc.M109.080317

Hoefs, S.J., F.J. van Spronsen, E.W. Lenssen, L.G. Nijtmans, R.J. Rodenburg, J.A. Smeitink, and L.P. van den Heuvel. 2011. NDUFA10 mutations cause complex I deficiency in a patient with Leigh disease. *Eur. J. Hum. Genet.* 19:270–274. http://dx.doi.org/10.1038/ejhg.2010.204

Jin, S.M., M. Lazarou, C. Wang, L.A. Kane, D.P. Narendra, and R.J. Youle. 2010. Mitochondrial membrane potential regulates PINK1 import and proteolytic destabilization by PARL. *J. Cell Biol.* 191:933–942. http://dx.doi.org/10.1083/jcb.201008084

Johnson, B.D., R.J. Schumacher, E.D. Ross, and D.O. Toft. 1998. Hop modulates Hsp70/Hsp90 interactions in protein folding. *J. Biol. Chem.* 273:3679–3686. http://dx.doi.org/10.1074/jbc.273.6.3679

Jung, S.Y., A. Malovannaya, J. Wei, B.W. O'Malley, and J. Qin. 2005. Proteomic analysis of steady-state nuclear hormone receptor coactivator complexes. *Mol. Endocrinol.* 19:2451–2465. http://dx.doi.org/10.1210/me.2004-0476

Jung, S.Y., Y. Li, Y. Wang, Y. Chen, Y. Zhao, and J. Qin. 2008. Complications in the assignment of 14 and 28 Da mass shift detected by mass spectrometry as in vivo methylation from endogenous proteins. *Anal. Chem.* 80:1721–1729. http://dx.doi.org/10.1021/ac7021025

Kampmueller, K.M., and D.J. Miller. 2005. The cellular chaperone heat shock protein 90 facilitates Flock House virus RNA replication in *Drosophila* cells. *J. Virol.* 79:6827–6837. http://dx.doi.org/10.1128/JVI.79.11.6827-6837.2005

Knott, A.B., G. Perkins, R. Schwarzenbacher, and E. Bossy-Wetzel. 2008. Mitochondrial fragmentation in neurodegeneration. *Nat. Rev. Neurosci.* 9:505–518. http://dx.doi.org/10.1038/nrn2417

Koch, R., R. Ledermann, O. Urwyler, M. Heller, and B. Suter. 2009. Systematic functional analysis of Bicaudal-D serine phosphorylation and intragenic suppression of a female sterile allele of BicD. *PLoS ONE*. 4:e4552. http://dx.doi.org/10.1371/journal.pone.0004552

LaJeunesse, D.R., S.M. Buckner, J. Lake, C. Na, A. Pirt, and K. Fromson. 2004. Three new *Drosophila* markers of intracellular membranes. *Biotechniques*. 36:784–788: 790.

Lazarou, M., D.R. Thorburn, M.T. Ryan, and M. McKenzie. 2009. Assembly of mitochondrial complex I and defects in disease. *Biochim. Biophys. Acta*. 1793:78–88. http://dx.doi.org/10.1016/j.bbamcr.2008.04.015

Ly, C.V., C.K. Yao, P. Verstreken, T. Ohyama, and H.J. Bellen. 2008. *straightjacket* is required for the synaptic stabilization of cacophony, a voltage-gated calcium channel α_1 subunit. *J. Cell Biol.* 181:157–170. http://dx.doi.org/10.1083/jcb.200712152

Manczak, M., B.S. Park, Y. Jung, and P.H. Reddy. 2004. Differential expression of oxidative phosphorylation genes in patients with Alzheimer's disease: implications for early mitochondrial dysfunction and oxidative damage. *Neuromolecular Med.* 5:147–162. http://dx.doi.org/10.1385/NMM:5:2:147

Marc, P., A. Margeot, F. Devaux, C. Blugeon, M. Corral-Debrinski, and C. Jacq. 2002. Genome-wide analysis of mRNAs targeted to yeast mitochondria. *EMBO Rep.* 3:159–164. http://dx.doi.org/10.1093/embo-reports/kvf025

Martín, M.A., A. Blázquez, L.G. Gutierrez-Solana, D. Fernández-Moreira, P. Briones, A.L. Andreu, R. Garesse, Y. Campos, and J. Arenas. 2005. Leigh syndrome associated with mitochondrial complex I deficiency due to a novel mutation in the NDUFS1 gene. *Arch. Neurol.* 62:659–661. http://dx.doi.org/10.1001/archneur.62.4.659

Mast, J.D., K.M. Tomalty, H. Vogel, and T.R. Clandinin. 2008. Reactive oxygen species act remotely to cause synapse loss in a *Drosophila* model of developmental mitochondrial encephalopathy. *Development*. 135:2669–2679. http://dx.doi.org/10.1242/dev.020644

McKenzie, M., E.J. Tucker, A.G. Compton, M. Lazarou, C. George, D.R. Thorburn, and M.T. Ryan. 2011. Mutations in the gene encoding C8orf38 block complex I assembly by inhibiting production of the mitochondria-encoded subunit ND1. *J. Mol. Biol.* 414:413–426. http://dx.doi.org/10.1016/j.jmb.2011.10.012

Morais, V.A., P. Verstreken, A. Roethig, J. Smet, A. Snellinx, M. Vanbrabant, D. Haddad, C. Frezza, W. Mandemakers, D. Vogt-Weisenhorn, et al. 2009. Parkinson's disease mutations in PINK1 result in decreased Complex I activity and deficient synaptic function. *EMBO Mol. Med.* 1:99–111. http://dx.doi.org/10.1002/emmm.200900006

Moriwaki, Y., Y.J. Kim, Y. Ido, H. Misawa, K. Kawashima, S. Endo, and R. Takahashi. 2008. L347P PINK1 mutant that fails to bind to Hsp90/Cdc37 chaperones is rapidly degraded in a proteasome-dependent manner. *Neurosci. Res.* 61:43–48. http://dx.doi.org/10.1016/j.neures.2008.01.006

Morris, A.A., J.V. Leonard, G.K. Brown, S.K. Bidouki, L.A. Bindoff, C.E. Woodward, A.E. Harding, B.D. Lake, B.N. Harding, M.A. Farrell, et al. 1996. Deficiency of respiratory chain complex I is a common cause of Leigh disease. *Ann. Neurol.* 40:25–30. http://dx.doi.org/10.1002/ana.410400107

Neckers, L. 2002. Heat shock protein 90 inhibition by 17-allylamino-17- demethoxygeldanamycin: a novel therapeutic approach for treating hormone-refractory prostate cancer. *Clin. Cancer Res.* 8:962–966.

Neckers, L. 2006. Chaperoning oncogenes: Hsp90 as a target of geldanamycin. *Handb. Exp. Pharmacol*. 172:259–277. http://dx.doi.org/10.1007/3-540-29717-0_11

Neumüller, R.A., F. Wirtz-Peitz, S. Lee, Y. Kwon, M. Buckner, R.A. Hoskins, K.J. Venken, H.J. Bellen, S.E. Mohr, and N. Perrimon. 2012. Stringent analysis of gene function and protein-protein interactions using fluorescently tagged genes. *Genetics*. 190:931–940. http://dx.doi.org/10.1534/genetics.111.136465

Ni, J.Q., L.P. Liu, R. Binari, R. Hardy, H.S. Shim, A. Cavallaro, M. Booker, B.D. Pfeiffer, M. Markstein, H. Wang, et al. 2009. A *Drosophila* resource of transgenic RNAi lines for neurogenetics. *Genetics*. 182:1089–1100. http://dx.doi.org/10.1534/genetics.109.103630

Nunnari, J., and A. Suomalainen. 2012. Mitochondria: in sickness and in health. *Cell*. 148:1145–1159. http://dx.doi.org/10.1016/j.cell.2012.02.035

Okiyoneda, T., H. Barrière, M. Bagdány, W.M. Rabeh, K. Du, J. Höhfeld, J.C. Young, and G.L. Lukacs. 2010. Peripheral protein quality control removes unfolded CFTR from the plasma membrane. *Science*. 329:805–810. http://dx.doi.org/10.1126/science.1191542

Osoegawa, K., and P.J. de Jong. 2004. BAC library construction. *Methods Mol. Biol.* 255:1–46.

Osoegawa, K., P.J. de Jong, E. Frengen, and P.A. Ioannou. 2001. Construction of bacterial artificial chromosome (BAC/PAC) libraries. *Curr. Protoc. Hum. Genet.* Chapter 5:Unit 5.15.

Owusu-Ansah, E., and U. Banerjee. 2009. Reactive oxygen species prime *Drosophila* haematopoietic progenitors for differentiation. *Nature*. 461 :537–541. http://dx.doi.org/10.1038/nature08313

Owusu-Ansah, E., A. Yavari, S. Mandal, and U. Banerjee. 2008. Distinct mitochondrial retrograde signals control the G1-S cell cycle checkpoint. *Nat. Genet.* 40:356–361. http://dx.doi.org/10.1038/ng.2007.50

Pagliarini, D.J., S.E. Calvo, B. Chang, S.A. Sheth, S.B. Vafai, S.E. Ong, G.A. Walford, C. Sugiana, A. Boneh, W.K. Chen, et al. 2008. A mitochondrial protein compendium elucidates complex I disease biology. *Cell*. 134:112–123. http://dx.doi.org/10.1016/j.cell.2008.06.016

Parks, A.L., K.R. Cook, M. Belvin, N.A. Dompe, R. Fawcett, K. Huppert, L.R. Tan, C.G. Winter, K.P. Bogart, J.E. Deal, et al. 2004. Systematic generation of high-resolution deletion coverage of the *Drosophila melanogaster* genome. *Nat. Genet.* 36:288–292. http://dx.doi.org/10.1038/ng1312

Poole, A.C., R.E. Thomas, L.A. Andrews, H.M. McBride, A.J. Whitworth, and L.J. Pallanck. 2008. The PINK1/Parkin pathway regulates mitochondrial morphology. *Proc. Natl. Acad. Sci. USA*. 105:1638–1643. http://dx.doi .org/10.1073/pnas.0709336105

Robinson, G.W., Y.H. Tsay, B.K. Kienzle, C.A. Smith-Monroy, and R.W. Bishop. 1993. Conservation between human and fungal squalene synthetases: similarities in structure, function, and regulation. *Mol. Cell. Biol.* 13:2706–2717.

Rubin, G.M., L. Hong, P. Brokstein, M. Evans-Holm, E. Frise, M. Stapleton, and D.A. Harvey. 2000. A *Drosophila* complementary DNA resource. *Science*. 287:2222–2224. http://dx.doi.org/10.1126/science.287.5461.2222

Ryder, E., F. Blows, M. Ashburner, R. Bautista-Llacer, D. Coulson, J. Drummond, J. Webster, D. Gubb, N. Gunton, G. Johnson, et al. 2004. The DrosDel collection: a set of P-element insertions for generating custom chromosomal aberrations in *Drosophila melanogaster*. *Genetics*. 167:797–813. http://dx.doi.org/10.1534/genetics.104.026658

Saada, A., R.O. Vogel, S.J. Hoefs, M.A. van den Brand, H.J. Wessels, P.H. Willems, H. Venselaar, A. Shaag, F. Barghuti, O. Reish, et al. 2009. Mutations in NDUFAF3 (C3ORF60), encoding an NDUFAF4 (C6ORF66)-interacting complex I assembly protein, cause fatal neonatal mitochondrial disease. *Am. J. Hum. Genet.* 84:718–727. http://dx.doi .org/10.1016/j.ajhg.2009.04.020

Shaner, N.C., R.E. Campbell, P.A. Steinbach, B.N. Giepmans, A.E. Palmer, and R.Y. Tsien. 2004. Improved monomeric red, orange and yellow fluorescent proteins derived from *Discosoma* sp. red fluorescent protein. *Nat. Biotechnol.* 22:1567–1572. http://dx.doi.org/10.1038/nbt1037

Stapleton, M., G. Liao, P. Brokstein, L. Hong, P. Carninci, T. Shiraki, Y. Hayashizaki, M. Champe, J. Pacleb, K. Wan, et al. 2002. The *Drosophila* gene collection: identification of putative full-length cDNAs for 70% of *D. melanogaster* genes. *Genome Res.* 12:1294–1300. http://dx.doi.org/ 10.1101/gr.269102

Strausberg, R.L., E.A. Feingold, L.H. Grouse, J.G. Derge, R.D. Klausner, F.S. Collins, L. Wagner, C.M. Shenmen, G.D. Schuler, S.F. Altschul, et al; Mammalian Gene Collection Program Team. 2002. Generation and initial analysis of more than 15,000 full-length human and mouse cDNA sequences. *Proc. Natl. Acad. Sci. USA*. 99:16899–16903. http://dx.doi.org/ 10.1073/pnas.242603899

Thibault, S.T., M.A. Singer, W.Y. Miyazaki, B. Milash, N.A. Dompe, C.M. Singh, R. Buchholz, M. Demsky, R. Fawcett, H.L. Francis-Lang, et al. 2004. A complementary transposon tool kit for *Drosophila melanogaster* using P and piggyBac. *Nat. Genet.* 36:283–287. http://dx.doi.org/ 10.1038/ng1314

Tong, C., T. Ohyama, A.C. Tien, A. Rajan, C.M. Haueter, and H.J. Bellen. 2011. Rich regulates target specificity of photoreceptor cells and N-cadherin trafficking in the *Drosophila* visual system via Rab6. *Neuron*. 71:447–459. http://dx.doi.org/10.1016/j.neuron.2011.06.040

Truscott, K.N., K. Brandner, and N. Pfanner. 2003. Mechanisms of protein import into mitochondria. *Curr. Biol.* 13:R326–R337. http://dx.doi.org/ 10.1016/S0960-9822(03)00239-2

Venken, K.J., Y. He, R.A. Hoskins, and H.J. Bellen. 2006. P[acman]: a BAC transgenic platform for targeted insertion of large DNA fragments in *D. melanogaster*. *Science*. 314:1747–1751. http://dx.doi.org/10.1126/ science.1134426

Venken, K.J., E. Popodi, S.L. Holtzman, K.L. Schulze, S. Park, J.W. Carlson, R.A. Hoskins, H.J. Bellen, and T.C. Kaufman. 2010. A molecularly defined duplication set for the X chromosome of *Drosophila melanogaster*. *Genetics*. 186:1111–1125. http://dx.doi.org/10.1534/genetics .110.121285

Verstreken, P., T.W. Koh, K.L. Schulze, R.G. Zhai, P.R. Hiesinger, Y. Zhou, S.Q. Mehta, Y. Cao, J. Roos, and H.J. Bellen. 2003. Synaptojanin is recruited by endophilin to promote synaptic vesicle uncoating. *Neuron*. 40:733–748. http://dx.doi.org/10.1016/S0896-6273(03)00644-5

Vogel, R.O., R.J. Janssen, C. Ugalde, M. Grovenstein, R.J. Huijbens, H.J. Visch, L.P. van den Heuvel, P.H. Willems, M. Zeviani, J.A. Smeitink, and L.G. Nijtmans. 2005. Human mitochondrial complex I assembly is mediated by NDUFAF1. *FEBS J.* 272:5317–5326. http://dx.doi.org/10.1111/j.1742-4658.2005.04928.x

Weihofen, A., B. Ostaszewski, Y. Minami, and D.J. Selkoe. 2008. Pink1 Parkinson mutations, the Cdc37/Hsp90 chaperones and Parkin all influence the maturation or subcellular distribution of Pink1. *Hum. Mol. Genet.* 17:602–616. http://dx.doi.org/10.1093/hmg/ddm334

Xiong, B., V. Bayat, M. Jaiswal, K. Zhang, H. Sandoval, W.L. Charng, T. Li, G. David, L. Duraine, Y.Q. Lin, et al. 2012. Crag is a GEF for Rab11 required for rhodopsin trafficking and maintenance of adult photoreceptor cells. *PLoS Biol*. 10:e1001438. http://dx.doi.org/10.1371/journal .pbio.1001438

Yamamoto, S., W.L. Charng, N.A. Rana, S. Kakuda, M. Jaiswal, V. Bayat, B. Xiong, K. Zhang, H. Sandoval, G. David, et al. 2012. A mutation in EGF repeat-8 of Notch discriminates between Serrate/Jagged and Delta family ligands. *Science*. 338:1229–1232. http://dx.doi.org/ 10.1126/science.1228745

Yan, L.J., R.L. Levine, and R.S. Sohal. 1997. Oxidative damage during aging targets mitochondrial aconitase. *Proc. Natl. Acad. Sci. USA*. 94:11168–11172. http://dx.doi.org/10.1073/pnas.94.21.11168

Yarosh, W., J. Monserrate, J.J. Tong, S. Tse, P.K. Le, K. Nguyen, C.B. Brachmann, D.C. Wallace, and T. Huang. 2008. The molecular mechanisms of OPA1-mediated optic atrophy in *Drosophila* model and prospects for antioxidant treatment. *PLoS Genet.* 4:e6. http://dx.doi.org/10.1371/journal .pgen.0040006

Yoneda, T., C. Benedetti, F. Urano, S.G. Clark, H.P. Harding, and D. Ron. 2004. Compartment-specific perturbation of protein handling activates genes encoding mitochondrial chaperones. *J. Cell Sci.* 117:4055–4066. http:// dx.doi.org/10.1242/jcs.01275

Young, J.C., I. Moarefi, and F.U. Hartl. 2001. Hsp90: a specialized but essential protein-folding tool. *J. Cell Biol.* 154:267–273. http://dx.doi .org/10.1083/jcb.200104079

Young, J.C., N.J. Hoogenraad, and F.U. Hartl. 2003. Molecular chaperones Hsp90 and Hsp70 deliver preproteins to the mitochondrial import receptor Tom70. *Cell*. 112:41–50. http://dx.doi.org/10.1016/S0092-8674(02)01250-3

Zhai, R.G., Y. Cao, P.R. Hiesinger, Y. Zhou, S.Q. Mehta, K.L. Schulze, P. Verstreken, and H.J. Bellen. 2006. *Drosophila* NMNAT maintains neural integrity independent of its NAD synthesis activity. *PLoS Biol.* 4:e416. http://dx.doi.org/10.1371/journal.pbio.0040416

Zhao, R., and W.A. Houry. 2007. Molecular interaction network of the Hsp90 chaperone system. *Adv. Exp. Med. Biol.* 594:27–36. http://dx.doi.org/ 10.1007/978-0-387-39975-1_3

Zhao, R., M. Davey, Y.C. Hsu, P. Kaplanek, A. Tong, A.B. Parsons, N. Krogan, G. Cagney, D. Mai, J. Greenblatt, et al. 2005. Navigating the chaperone network: an integrative map of physical and genetic interactions mediated by the hsp90 chaperone. *Cell*. 120:715–727. http://dx.doi.org/ 10.1016/j.cell.2004.12.024

Zurita Rendón, O., and E.A. Shoubridge. 2012. Early complex I assembly defects result in rapid turnover of the ND1 subunit. *Hum. Mol. Genet.* 21:3815–3824. http://dx.doi.org/10.1093/hmg/dds209